



Article

Defining Regional and Local Sediment Sources in the Ancestral Colorado River System: A Heavy Mineral Study of a Mixed Provenance Unit in the Fish Creek-Vallecito Basin, Southern California

Paula McGill ^{1,*}, Uisdean Nicholson ², Dirk Frei ³  and David Macdonald ⁴ ¹ HM Research Norway AS, Tananger, 4056 Stavanger, Norway² School of Energy, Geoscience, Infrastructure and Society, Heriot-Watt University, Edinburgh EH14 4AS, UK³ Department of Earth Science, University of the Western Cape, Private Bag X17, Cape Town 7535, South Africa⁴ School of Geosciences, University of Aberdeen, Aberdeen AB24 3UE, UK

* Correspondence: paula.hmresearch@gmail.com

Abstract: The Colorado River has flowed across the dextral strike-slip plate boundary between the North American and Pacific plates since the latest Miocene or earliest Pliocene. The Fish Creek-Vallecito Basin (FCVB) lies on the Pacific Plate in southern California, dextrally offset from the point where the modern Colorado river enters the Salton Trough; it contains a record of ancestral Colorado River sedimentation from 5.3–2.5 Ma. The basin stratigraphy exhibits a changing balance between locally derived (L-Suite) and Colorado River (C-Suite) sediments. This paper focuses on the Palm Springs Group (PSG), a thick fluvial and alluvial sequence deposited on the upper delta plain (between 4.2–2.5 Ma) when the Colorado was active in the area, allowing the detailed examination of the processes of sediment mixing from two distinct provenance areas. The PSG consists of three coeval formations: 1) Canebrake Conglomerate, a basin margin that has coarse alluvial fan deposits derived from surrounding igneous basement; 2) Olla Formation, fan-fringe sandstones containing L-Suite, C-Suite, and mixed units; and 3) Arroyo Diablo Formation, mineralogically mature C-Suite sandstones. Stratigraphic analysis demonstrates that the river flowed through a landscape with relief up to 2000 m. Satellite mapping and detailed logging reveal a variable balance between the two suites in the Olla Formation with an apparent upward increase in L-Suite units before abrupt cessation of Colorado sedimentation in the basin. Stable heavy mineral indices differentiate L-Suite (high rutile:zircon index: RZi 40–95) from C-Suite (RZi: 0–20). Both suites have garnet:zircon index (GZi) and apatite:tourmaline index (ATi) mostly above 50, although many L-suite and mixed Olla samples have much lower ATi (20–50), suggesting that the distal floodplain was wet and the local sediment had a longer residence time there, or went through several cycles of erosion and redeposition. Heavy mineral analysis, garnet geochemical analysis, and detrital zircon U-Pb age spectra allow us to quantify the amount of mixing from different sediment sources. These data show that about 30% of the mixed units are derived from the Colorado River and that up to 20% of the L-Suite is also derived from the Colorado River, suggesting that there was mutual cannibalisation of older deposits by fluvial channels in a transitional area at the basin margin. Although this study is local in scope, it provides an insight into the extent and nature of sediment mixing in a two-source system. We conclude that most ‘mixing’ is actually interbedding from separate sources; true mixing is facilitated by low subsidence rates and the rapid migration of fluvial channels.

Keywords: sediment flux; axial and lateral supply; California; Colorado River; heavy minerals; palaeotopography



Citation: McGill, P.; Nicholson, U.; Frei, D.; Macdonald, D. Defining Regional and Local Sediment Sources in the Ancestral Colorado River System: A Heavy Mineral Study of a Mixed Provenance Unit in the Fish Creek-Vallecito Basin, Southern California. *Geosciences* **2023**, *13*, 45. <https://doi.org/10.3390/geosciences13020045>

Academic Editors: Shane Tyrrell and Jesus Martinez-Frias

Received: 22 August 2022

Revised: 27 January 2023

Accepted: 28 January 2023

Published: 31 January 2023



Copyright: © 2023 by the authors. Licensee MDPI, Basel, Switzerland. This article is an open access article distributed under the terms and conditions of the Creative Commons Attribution (CC BY) license (<https://creativecommons.org/licenses/by/4.0/>).

1. Introduction

The Fish Creek-Vallecito Basin (FCVB) lies on the Pacific Plate in southern California, southwest of the Salton Sea (Figure 1A). The basin is dextrally offset by the San Andreas

fault from the point where the modern Colorado River enters the Salton Trough [1]. In the latest Miocene and Early Pliocene, the FCVB was located directly west of this entry point [2]. Because of this, the basin contains the most complete record of early ancestral Colorado River sedimentation anywhere in California [3–9]. This sedimentary record is important for the geological history of the western cordillera, representing the first sedimentation from the elevated Colorado Plateau to reach the Pacific margin [2,10]. The FCVB also holds one of the richest, most varied fossil records of the past 7 Ma in North America [11]. Globally, the basin is significant as a record of one of the very few great rivers to deposit its delta across a strike-slip plate boundary, along with the Orinoco [12] and the Amur [13,14]; it is also unique in that the delta is partly deposited across a spreading ridge [15].

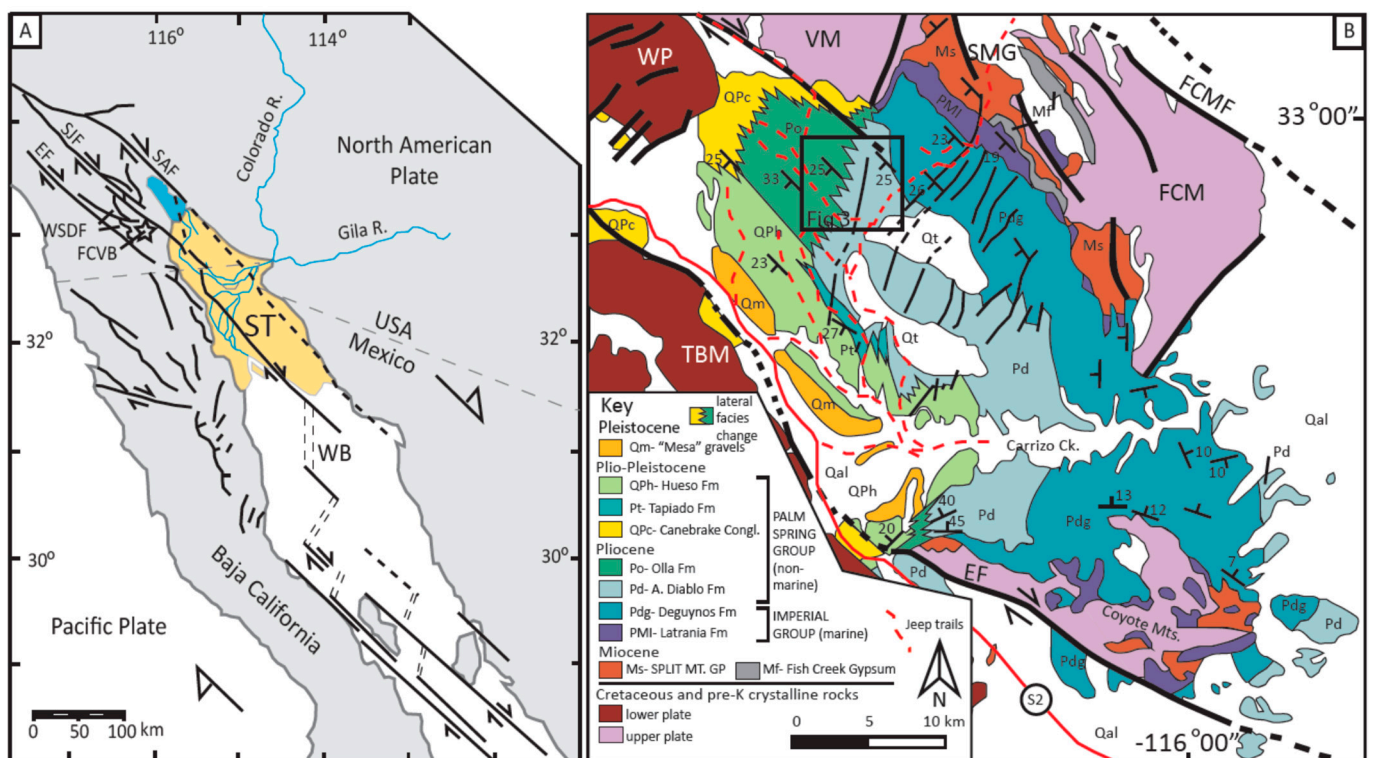


Figure 1. (A) regional tectonic elements map (after Dorsey et al. [8]) showing locations of major faults of the North America-Pacific (NAM:PAC) plate boundary system in the northern Gulf of California and the Salton Trough (ST). Orange colour shows extent of modern Colorado sands in the Salton Trough; star shows location of the Fish Creek-Vallecito Basin (FCVB). (B) Geological map of the FCVB (after Dorsey et al. [8,16]) showing the stratigraphic relationship of the Olla Formation to the Arroyo Diablo and Canebrake formations. Note the small outcrop of Olla Formation in the western Coyote Mountains. EF—Elsinore Fault; FCM—Fish Creek Mountains; FCMF—Fish Creek Mountain Fault; SMG—Split Mountain Gorge; TBM—Tierra Blanca Mountains; VM—Vallecito Mountains; WP—Whale Peak.

The Colorado deposited a large delta in the FCVB, starting at either 5.3 Ma [8] or 4.8–4.63 Ma [17]; the timing is disputed (see discussion by Dorsey et al. [18] and the reply from Crow et al. [19]). Colorado River sedimentation ended in the basin 2.3 Ma ago [8]. The stratigraphic record of the basin gives a complete history of the basin from the Miocene, with locally derived sedimentation Split Mountain Group, through the arrival of Colorado sands and the deposition of a substantial prodelta, delta slope, and lower delta plain (Imperial Group), followed by a thick fluvial and alluvial sequence deposited on the upper delta plain (Palm Springs Group); this history is summarised in Table 1.

Table 1. Summary of FCVB stratigraphy from various sources, principally [8] (see text); formations of interest are highlighted. The highlighted section represents the stratigraphy relevant to this study.

Group	Formation	Member	Thickness (m)	Age (Ma)	Lithology	Interpretation	Notes
Pleistocene not assigned to a group	Mesa		> 100	0.126–0	Gravels	Fluvial	All locally derived
	Bow Willow Beds		5–30	0.9–0.126	Sst, conglom., & minor lst.	Fluvial and lacustrine	Locally derived; abundant paleosols
Palm Springs	Hueso	Fanning-dip Interval (200 m)	52	2.8–0.9	Sandstone	Fluvial	For a discussion of the Fanning-dip Interval, see Dorsey et al. [16].
	Tapiado		375	2.8–2.0	Mudstone	Lacustrine	Contains tuffs
	Diablo		2520	4.2–2.8	Sandstone	Fluvial—delta plain	Colorado River provenance
	Olla						Colorado & local provenance
	Canebrake		c. 2700	c. 4.3–2.0	Conglomerate	Alluvial fan	Local derivation
Imperial	Deguynos	Camel's Head	325	4.2–4.09	Mudstone & sandstone	Prograding delta front	Mixed provenance
		Yuha	350	4.49–4.2			
		Mud Hills	400	5.1–4.49	Mudstone	Prodelta	
	Latrania	Wind Caves	150	5.33 or 4.8	Sandstone	Turbidites	First Colorado sands
		Upper Megabreccia	0–50	5.4	Breccia	Mass flow	Instantaneous event
		Lycium	140	6.27–5.4	Sandstone & mudstone	Turbidites	Local provenance
	Fish Creek Gypsum	0–>65		Gypsum	Marginal marine	Adjacent to FCVB to north	
Split Mountain (age ranges extrapolated from modelled sedimentation rates)	Lower Megabreccia	Split Mountain		c. 6.4	Breccia	Subaerial rock avalanche	Instantaneous event
		Red & Grey					
	Elephant Trees	Conglomerate		500	Sandstone & conglomerate	Alluvial fan & fluvial	Local provenance; bed thickness variable (0–200 m)
		Lower Tan Sst.					
Alverson Andesite			22–14	Olivine basalt and andesite	Extension	0–120 m thick in FCVB area (Woodard 1974)	
Red Rock			>22	Pebbly Sst.	?Fluvial		

In this paper, we use field observations and the techniques of stratigraphic analysis and heavy mineral analysis (HMA) to understand the provenance of the fluvial unit (Palm Springs Group) defined by Dibblee [3] and Winker [20], concentrating on the lower part of the group. This comprises three coevally deposited formations: the Canebrake Conglomerate Formation on the basin margin, the Arroyo Diablo Formation covering most of the basin, and the Olla Formation which lies between the other two units and shares some of the characteristics of each. The sediments overlying these three formations (Hueso and Tapiado formations) represent the time when the Colorado delta migrated farther south, and Colorado sedimentation ceased in the FCVB.

The changing relationship of the Olla Formation with the other formations of the Palm Springs Group is important in understanding the behaviour of the Colorado River through time. This formation varies in outcrop width and provenance, allowing us to assess changes in the sediment flux to the basin, which was controlled by both the Colorado River and local influences.

The FCVB forms a beautifully exposed natural laboratory for studying the balance between a far-field-supplied (extrabasinal) sediment routing system [21] and local intra- and peri-basinal sources. In this paper, we explore the recognition of multiple provenances, the style of interbedding and mixing, the evolution of the multiply supplied system through time, and a discussion of climatic, sedimentological, paleotopographical, and tectonic controls on sedimentation.

The study is also important for determining whether the bed-load of tributary rivers can become mixed with that of the trunk stream, as in the case of the Rhine system [22]; whether they stay distinct, with the trunk stream delivering material to its delta without significant additions from tributaries, as is the case for the Amur River of NE Asia [23]; or whether it is somewhere in between these end members.

2. Geological Background

The Fish Creek-Vallecito Basin lies in the hanging wall of the West Salton Detachment Fault (WSDF), a low-angle extensional detachment which trends roughly SSE-NNW, with a downthrow towards the east (Figure 1B; [24,25]). The WSDF is one of a family of oblique extensional faults that formed as a result of the Miocene opening of the Gulf of California [1]. Flooding of the northernmost 500 km, including the FCVB, had occurred by c. 6.3 Ma [26]. The basin lies between the Elsinore and San Felipe faults, both dextral strike-slip faults, west of and sub-parallel to the San Andreas Fault. The WSDF is offset dextrally by the San Felipe Fault and continues north to the San Jacinto Fault Zone [27].

The basin is oriented NW–SE and has the form of a complex plunging monocline (Figure 1B) with a general SW-directed dip of 25–30°; the northern and southern ends are folded with plunges directed to the NW.

Elements of the basin fill are unconformable on the basement in the Vallecito Mountains (NW), the Fish Creek Mountains (N), and the Coyote Mountains (SE). The stratigraphy of the basin (Figure 2 and Table 1) spans the Miocene to the Early Pleistocene [1,6,8,18,27]. The basin fill has been divided into three major lithostratigraphic groups (Table 1).

2.1. Split Mountain Group

The Split Mountain Group consists of a sequence of immature clastic sediments deposited in a subaerial environment overlying Cretaceous granitoids and pre-Cretaceous metamorphic rocks. The unconformity defines significant irregular topography and sediments were derived locally with deposition in alluvial fans, braided streams, debris flows and very large rock avalanches, including alluvial and fluvial conglomerates and sandstones of the Red Rock and Elephant Trees formations. This sequence also includes the Alverson Formation volcanics [28] and the Lower Megabreccia of variable thickness [8], interpreted as a subaerial Sturztrom deposit. The volcanics and the Megabreccia indicate that the northern Gulf of California was tectonically active at the time, with elements of both strike-slip faulting and extension [1,26,29,30].

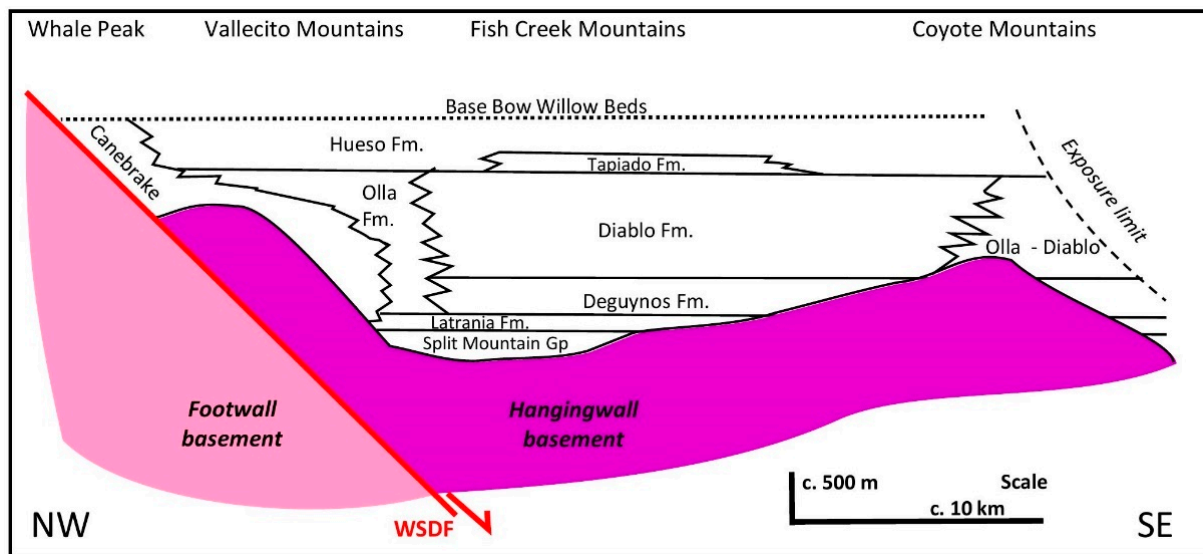


Figure 2. Stratigraphic cartoon showing a dip-normal view of the stratigraphic relationship of sedimentary formations to each other and to the basement topography, which exceeds 2 km thickness in the hangingwall of the WSDF. Note that the hangingwall topography was not completely overtopped until Olla/Arroyo Diablo times and the footwall topography persisted throughout the sedimentation history of the basin.

2.2. Imperial Group

The Imperial Group (Upper Miocene-Pliocene) comprises marine sandstone and mudstone deposited in a prodelta setting with about 150 m of L-Suite turbidites at the base. Above these, there is a rapid transition to C-Suite turbidites, indicating the Colorado-derived sediment flux overwhelms that of local sources [2,6]. C-Suite sands dominate the rest of this group, although L-Suite beds are occasionally present.

2.3. Palm Springs Group

The Palm Springs Group (Pliocene-Pleistocene) records fluvial sedimentation in the ancestral Colorado River (4.3–2.8 Ma) up to the abandonment of this pathway and replacement by locally derived streams (2.8–0.9 Ma). The persistence of local sediment supply (L Suite; arkosic) and Colorado River supply (C Suite; quartzose) is well known [6,20,31,32]. Not only are the two suites easy to distinguish in the field using hand specimens, but there is a clear petrographic distinction [6]. The Hueso and Tapiado formations contain no Colorado material, but the three lowest formations are coeval, and two of them contain abundant Colorado sand; these three constituent formations of the group are distinguished by composition and facies:

- The Canebrake Conglomerate Formation mantles the whole of the western basin margin, unconformably overlying Cretaceous basement and in contact with footwall basement in the hanging wall of the WSDF. It comprises locally derived, coarse-grained alluvial fan deposits. These local deposits (L-suite of Winker & Kidwell [6]) have a clear provenance in the surrounding diorite and granodiorite basement [33]. It interfingers with the Olla Formation to the southeast in a relatively narrow transition zone;
- The fluvial Olla Formation has both L-suite and C-suite units, interbedded on a scale of metres to tens of metres;
- The fluvial Arroyo Diablo Formation interfingers with the Olla Formation in the NW; it also is composed of mineralogically mature, pale yellowish buff, well-sorted, fine-medium sandstones with a heavy mineral composition very similar to that of the modern Colorado River [9]. They are thought to have a Colorado River provenance and have been defined as the C-suite by Winker & Kidwell [6].

The sedimentology of the FCVB has been well-described [6,20,32], and there is an excellent chronostratigraphic framework [8] with more recent modifications by Crow et al. [17]. The stratigraphy and depositional environments of the basin are summarised in Table 1. The delta plain sedimentation was studied by Winker [20], who drew a very clear distinction between the Arroyo Diablo and Olla “members” (now formations). He described the Arroyo Diablo as homogeneous across the basin, comprising yellowish-buff, friable, well-sorted, C-Suite sandstones in metre-scale units up to 10 m thick with thinner interbedded units of reddish-brown mudstone. Detailed logs show that sand units are cross-bedded or cross-laminated, with planar and convolute bedding also commonly observed. He described 5–10 m scale fining upward units with sharp erosive bases. There are some interbedded L-Suite units, particularly in the area of Fish Creek Wash. The Olla Formation is described as interbedded C- and L-Suite units; the C-Suite beds were near-identical to the Arroyo Diablo, although the bases of upward fining cycles were more likely to contain L-Suite material. L-Suite units in the Olla are greenish grey and better cemented than the C-Suite units; they are dominated by low angle cross-beds, ripple cross lamination, and scour-and-fill structures. Winker went on to say that “*The lateral boundary between the Olla and Diablo members [sic] is intergradational and difficult to define precisely*”, but also stated that the definition of the Olla Formation is the presence of at least 20% ‘L-suite’ sandstone and siltstone beds. He favoured deposition in a meandering river system but did not discount the possibility of a high bed-load braided system.

The transition zone between the Olla and Arroyo Diablo formations has never been rigorously defined and may have relevance to other areas. The boundary between the two formations is generally shown as a zigzag line on both maps and logs, indicating interfingering of the two units [3,16]. Previous studies in the FCVB have shown that there is a clear petrographic and textural difference between locally derived sediments and those from the Colorado River [6]. This is also evident from heavy mineral studies, particularly from stable mineral assemblages [9] and from detrital zircons [7,9]. These data have been interpreted to show progressive erosion of the Colorado Plateau since the Miocene.

3. Methodology

3.1. Field Work and Remote Observation

The results presented here are based on five field seasons from 1996–2011. Field work concentrated on the section through Split Mountain Gorge and along Fish Creek Wash to the lower boundary of the Hueso Formation. Observations were also made on the NW flank of the Coyote Mountains. Detailed sedimentological logs were measured throughout the basin [33,34], but in this paper, we focus on the 34 sections in the vicinity of the Olla-Arroyo Diablo transition zone (Figure 3; Table 2). These logs record grain size, sedimentary structures, and any local thickness changes. Samples (minimum 500 g) were collected from these sections and also from individual localities close to the basin margin for petrographic, heavy mineral, and single grain geochemical and isotope analyses. Sampling was carried out to target both C- and L-suites, as defined by Winker [20], as well as paler yellow-green units, which may be a mixture of the two provenances.

The correlation of measured sections and recognition of bed thickness variation was facilitated using Google Earth, where the distinction between C- and L-suites is quite clear. The tilt function was used to study down-dip views of sections of the Olla/Arroyo Diablo stratigraphy and across the transition zone between the two formations. Google Earth was also used to study the onlap relations of the basin fill to basement in the Vallecito, Fish Creek, and Coyote mountains.

3.2. Heavy Mineral Analysis

Heavy mineral analysis allows for a detailed insight into the provenance history of the basin. This technique has been used as a tool for provenance studies since Thürach [35] and was applied successfully throughout the first half of the 20th Century [36–39]. More recent studies have developed a systematic methodology based on an inclusive understanding

of sedimentary and diagenetic processes and how they can impact on a heavy mineral provenance signature [40–42].

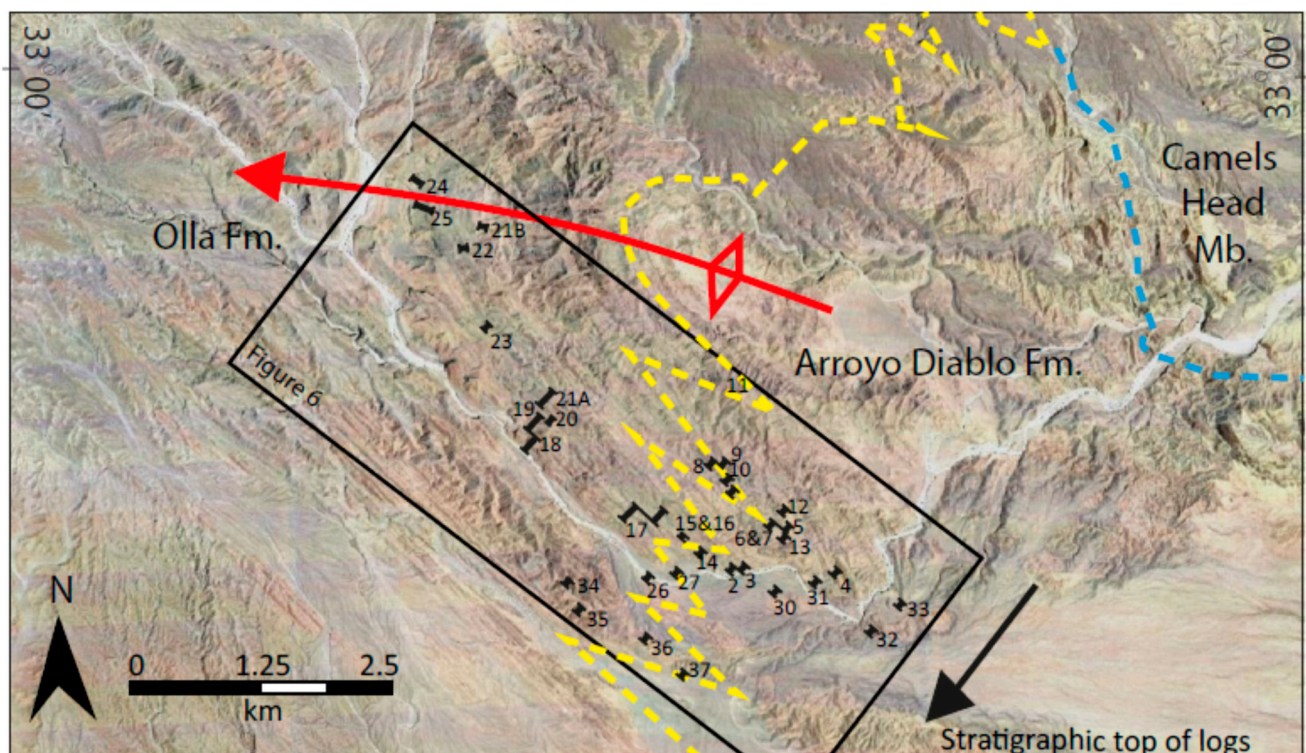


Figure 3. Location of measured sections and sampling sites in the area of western Fish Creek Wash: Google Earth image overlain by geological elements—the axial trace of the Fish Creek Anticline (red), the approximate location of the transition zone between the Olla and Arroyo Diablo formations (yellow), and the approximate location of the boundary between the Arroyo Diablo Formation and the Camels Head Member (blue). Note the distinction between green L-suite beds and buff C-suite units which is very clear on the SW limb of the Fish Creek Anticline.

Samples collected at the outcrop were disaggregated using a sonic bath and sieved, with the 125–63 μm fraction retained for further processing. This grain size fraction was selected in order to minimize the effects of hydraulic sorting. The heavy mineral component was separated from this dried fraction using bromoform (SG: 2.89) to remove the light (quartzo-feldspathic) minerals. The heavy fraction was collected in filter paper funnel, dried, and mounted evenly onto a glass slide using Canada balsam (refractive index 1.5). Samples were analysed based on the ribbon counting method of Mange and Maurer [43]. Grain counting provides an overview of the heavy mineral assemblages. Ratios of stable mineral pairs were then calculated in order to reduce the effects of hydrodynamic properties on some of the heavy mineral population [44] and the effects of burial diagenesis [44,45]. Based on the results of the preliminary count, certain mineral species were identified for further analysis. The varietal techniques used here were: garnet geochemistry [46] and detrital zircon U-Pb dating [47,48]. Individual mineral grains to be studied using these methodologies were picked from a portion of the heavy mineral residue and placed on a dry thin section, using a microscope for identification and a pin for separation. The garnets and zircons selected were placed on double-sided tape, mounted on separate slides for analysis: 65 grains per sample for garnet analysis and 150 zircon grains per sample for detrital zircon dating. These numbers are standard for these types of analysis and are sufficient to cover all compositions and age ranges.

Table 2. Aggregate thickness and percentage of each facies in each section; last column shows percentage of C Suite sand as a percentage of total sand. Yellow text highlight represents C-suite and green text highlight represents L-suite.

Section # (Figures 4 and 6)	Aggregate Thicknesses for Each Section (m)						Percentages of Each Facies by Section						C Suite as a % Total Sand	
	Section Length	Buff sst (C Suite)	Green sst (L Suite)	Green sst & silt (L)	Mixed (L & C)	Siltstone	Red Mudstone	Buff sst (C Suite)	Green sst (L Suite)	Green sst & Silt (L)	Mixed (L & C)	Siltstone		Red Mudstone
1	46.26	16.83	7.58	11.96	0.00	0.61	9.29	36.40	16.40	25.90	0.00	1.30	20.10	46
2	11.82	2.28	0.00	0.00	4.81	2.06	2.67	19.30	0.00	0.00	40.70	17.40	22.60	32
3	10.30	1.52	5.05	0.00	2.02	0.61	1.11	14.80	49.00	0.00	19.60	5.90	10.80	18
4	7.98	1.47	0.00	2.46	0.00	0.00	4.04	18.40	0.00	30.80	0.00	0.00	50.60	37
5	7.07	2.12	0.00	3.13	0.00	0.00	1.82	30.00	0.00	44.30	0.00	0.00	25.70	40
6 & 7	13.64	6.20	4.04	0.61	0.00	1.49	1.29	45.50	29.60	4.50	0.00	10.90	9.50	57
8	16.16	7.25	2.63	1.82	0.00	0.10	4.36	44.90	16.30	11.30	0.00	0.60	27.00	62
9	9.39	5.84	0.00	2.02	0.00	0.00	1.54	62.20	0.00	21.50	0.00	0.00	16.40	74
10	11.52	5.56	0.00	3.64	0.00	0.40	1.92	48.30	0.00	31.60	0.00	3.50	16.70	60
11	15.56	5.76	1.31	3.33	0.00	0.51	4.65	37.00	8.40	21.40	0.00	3.30	29.90	55
12	9.70	4.55	1.27	0.81	0.00	0.00	3.07	46.90	13.10	8.40	0.00	0.00	31.60	69
13	4.24	2.32	0.00	0.61	0.00	0.91	0.40	54.70	0.00	14.40	0.00	21.50	9.40	79
14	11.60	8.36	0.00	2.22	0.00	0.00	1.01	72.10	0.00	19.10	0.00	0.00	8.70	79
15 & 16	6.67	1.82	3.33	0.00	0.00	1.01	0.51	27.30	49.90	0.00	0.00	15.10	7.60	35
17	32.42	23.35	2.71	4.55	0.00	0.30	1.52	72.00	8.40	14.00	0.00	0.90	4.70	76
18B	43.43	34.24	0.00	0.61	3.74	2.63	2.22	78.80	0.00	1.40	8.60	6.10	5.10	89
19	19.60	5.90	7.33	0.00	0.00	4.55	1.82	30.10	37.40	0.00	0.00	23.20	9.30	45
20	11.72	1.52	0.40	0.00	4.95	2.42	2.42	13.00	3.40	0.00	42.20	20.60	20.60	22
21A	38.99	15.05	9.60	1.62	1.52	11.21	0.00	38.60	24.60	4.20	3.90	28.80	0.00	54
21B	26.87	6.40	2.12	14.34	2.42	0.00	1.58	23.80	7.90	53.40	9.00	0.00	5.90	25
22	16.16	6.18	0.00	5.76	3.58	0.65	0.00	38.20	0.00	35.60	22.20	4.00	0.00	40
23	19.80	7.68	0.00	5.25	1.31	4.75	0.81	38.80	0.00	26.50	6.60	24.00	4.10	54
24	32.32	15.90	0.00	0.00	5.21	11.11	0.10	49.20	0.00	0.00	16.10	34.40	0.30	75

Table 2. Cont.

Section # (Figures 4 and 6)	Aggregate Thicknesses for Each Section (m)						Percentages of Each Facies by Section						C Suite as a % Total Sand	
	Section Length	Buff sst (C Suite)	Green sst (L Suite)	Green sst & silt (L)	Mixed (L & C)	Siltstone	Red Mudstone	Buff sst (C Suite)	Green sst (L Suite)	Green sst & Silt (L)	Mixed (L & C)	Siltstone		Red Mudstone
25	39.39	10.63	8.99	1.01	7.47	9.31	1.98	27.00	22.80	2.60	19.00	23.60	5.00	38
26	11.01	10.30	0.00	0.00	0.00	0.00	0.71	93.60	0.00	0.00	0.00	0.00	6.40	100
27	22.83	17.37	0.61	0.00	0.00	1.72	3.13	76.10	2.70	0.00	0.00	7.50	13.70	97
30	24.95	11.74	1.33	0.00	3.94	1.92	6.02	47.10	5.30	0.00	15.80	7.70	24.10	69
31	10.61	5.25	1.41	0.00	0.00	0.10	3.84	49.50	13.30	0.00	0.00	0.90	36.20	79
32	10.71	6.67	0.71	0.00	0.00	0.61	2.73	62.30	6.60	0.00	0.00	5.70	25.50	90
33	21.62	14.71	0.65	0.00	2.12	0.81	3.33	68.00	3.00	0.00	9.80	3.70	15.40	84
34	21.41	17.90	0.00	0.20	1.35	0.61	1.35	83.60	0.00	0.90	6.30	2.80	6.30	92
35	42.83	32.36	0.00	0.20	4.34	0.87	5.05	75.60	0.00	0.50	10.10	2.00	11.80	88
36	19.39	15.15	0.00	1.11	0.00	0.81	2.32	78.10	0.00	5.70	0.00	4.20	12.00	93
37	30.81	19.19	0.71	1.11	2.42	0.61	6.77	62.30	2.30	3.60	7.90	2.00	22.00	82
Total/Ave %	678.77	349.37	61.78	68.36	51.21	62.67	85.37	51.50%	9.10%	10.10%	7.50%	9.20%	12.60%	66

Garnet geochemistry analysis was carried out using a MICROSCAN MK5 (Cambridge Scientific Instruments Ltd., London, UK) Electron Microprobe. The energy dispersive analysis system is a Link Analytical AN10/25S, and analyses were acquired and processed with the Links ZAF4/FLS program. Conditions for the analysis were accelerating voltage of 15 KV, a takeoff angle of 75°, a probe current of approximately 3.0 nA (approx. 2.2 nA on Cobalt Standard), a beam diameter of approximately 5 microns, and a Livetime of 30 s.

The detrital zircon U-Pb dating was carried out using an ablation-single collector-magnetic sectorfield-inductively coupled plasma-mass spectrometry (LA-SF-ICP-MS) at the Central Analytical Facility at Stellenbosch University, South Africa. The equipment used was Thermo Finnigan Element2 mass spectrometer coupled with a NewWave UP213 laser ablation system. The age data presented here were obtained by single spot analyses with a spot diameter of 30 µm and a crater depth of approximately 15–20 µm, corresponding to an ablated zircon mass of approximately 150–200 ng. The methods employed for analysis and data processing are described in detail by Gerdes and Zeh [49] and Frei and Gerdes [50]. For quality control, the Plešovice [50,51] and M127 [52,53] zircon reference materials were analysed. Full analytical details and the results for all quality control materials analysed are reported in the Supplementary Materials. Calculation of concordia ages and plotting of concordia diagrams was performed using Isoplot/Ex 3.0 [54].

4. Results

4.1. Field Work and Remote Observation—Stratigraphic Analysis

It has been suggested that the basin fill has been repeated by thrust faults related to the Earthquake Valley Fault [17], although this has been disputed [18]. Crow et al. [17] reported finding thrust flats at three stratigraphic intervals: in the Wind Caves Member; in the Yuha and Camels Head members; and in the lower part of the Olla Formation. Recent work on the Deguynos Formation [55] stated that “*we find no noticeable evidence of the major fault zones cutting the well-exposed outcrops in our area of study*”. During our work in the basin, which included detailed logging across the other two reported faulted intervals, we found no evidence of large-scale faulting in either the Wind Caves Member [33] or the Olla Formation [33,34]. For these reasons, we do not believe that there has been large-scale stratal repetition and treat the basin fill as a single coherent entity.

The starting point for the stratigraphic analysis was to use satellite images via Google Earth and the published geologic map of Dorsey et al. [16] to investigate the field relationships (summarised in Figure 1B). The stratigraphic boundaries can be directly observed over most of the basin with the exception of mesas of Quaternary terrace deposits in the north-central part of the basin (East, Middle, South, and West mesas) and Carrizo Creek, a ribbon of Quaternary fluvial deposits, running through the south-central part of the basin. The stratigraphy of the basin fill can be traced without interruption through the outcrop of these Quaternary units. The continuity of the base and top of the Olla/Diablo formations are striking. The lower boundary can be traced SE from the onlap of Olla onto the Vallecito Mountains, through East Mesa, across Carrizo Creek, to onlap of Arroyo Diablo onto the Coyote Mountains (Figure 4). The upper boundary can also be traced across the basin, although it is disrupted by minor N-S faults in the central part of the basin.

At the NW end of the basin, the Olla Formation is not seen in direct contact with basement anywhere. However, from the detailed map in Dorsey et al. ([16]; Figure 3 therein), it can be seen that bedding in the Olla Formation passes directly into the Canebrake Conglomerate, striking directly onto the basement of the Vallecito Mountains. Where the Canebrake Conglomerate is equivalent to the Hueso Formation, stratigraphically above the Olla, it rests directly on the WSDF. It is also worth noting that the lacustrine Tapiado Formation only overlies the Arroyo Diablo Formation; its gradational edge with the Hueso Formation is almost exactly counterposed with the Olla–Arroyo Diablo boundary below.

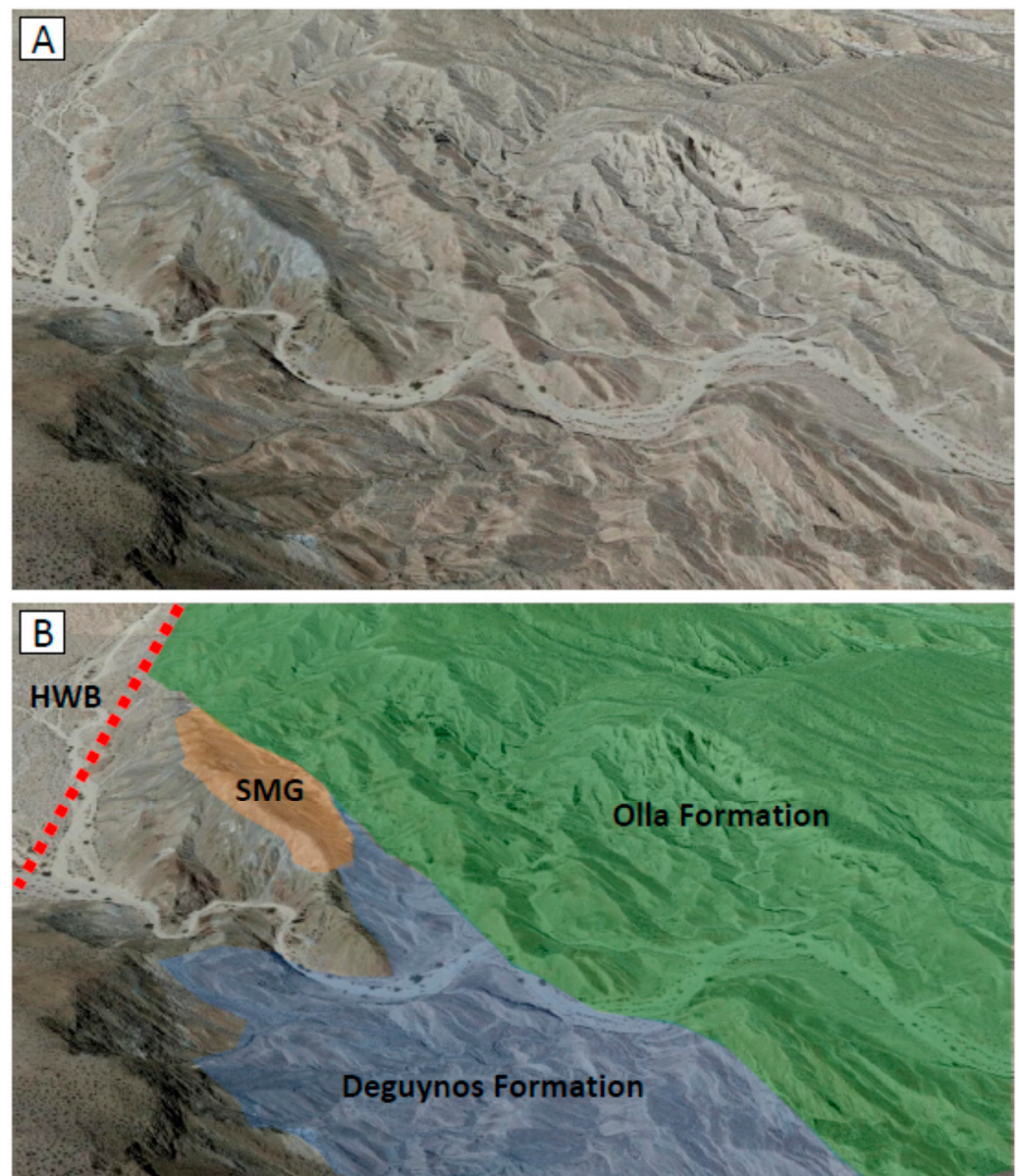


Figure 4. Oblique image from Google Earth showing onlap of the Olla Formation onto the western Coyote Mountains. The view is towards the WNW tip of the Coyote Mountains at Sin Nombre Canyon ($32^{\circ}50'06''$ N, $116^{\circ}09'21''$ W; elevation 276 m; view to azimuth 260° ; camera altitude 855 m; image is approximately 1 km wide across the middle ground of this view). (A) Uninterpreted image. (B) Interpreted image showing hanging wall basement (HWB—dark rocks to left of image, unshaded); this is overlain by a patch of Split Mountain Group (SMG—mid-grey in the uninterpreted view; shaded orange). The overlying Deguynos and Olla Formations are well-bedded and conformable with dips towards the NNW at about 40° . The Deguynos Formation (pale brown, shaded blue) rests directly on basement and oversteps onto the Split Mountain Group outcrop; it is overlapped in turn by the Olla Formation (light greyish brown, shaded green) which oversteps the Split Mountain Group to rest directly on basement.

These observations imply that:

1. The Olla–Arroyo Diablo unit is a coherent package in a relatively undisturbed unconformable relationship with basement on both sides of the basin. This suggests that Winker and Kidwell's [56] possibility of independent movement of the Coyote Mountains with respect to the Vallecito and Fish Creek Mountains during post-depositional

tectonics is probably untenable (their Figure 14, Alternative 1). We would, however, support their Alternative 2—rotation of the FCVB as a single entity.

2. The pre-depositional topography of the hanging wall block was not overtopped until the end of deposition of the Olla–Arroyo Diablo formations (Figure 2).
3. The restriction of the lacustrine Tapiado Formation to the area previously occupied by the Arroyo Diablo Formation may indicate that the Olla Formation and overlying parts of the Hueso Formation were deposited on a slope.

4.2. Field Work and Remote Observation—Sedimentology

Data collection was focused on the transition zone between the Olla and Arroyo Diablo formations, where 34 sections were measured, varying from 4–43 m (average 20 m, aggregate length 679 m). The data are presented in Figure 5 and summarised in Figure 6 and Table 2, with a full correlation panel shown in Supplementary Data (Figure S1). We recognise six facies associations, defined on grain size and provenance:

1. C-Suite sandstone;
2. L-suite sandstone;
3. L-Suite sandstone with interbedded black siltstone;
4. Black siltstone, dominantly associated with L-Suite;
5. Mixed C- and L-Suite sandstone;
6. Red mudstone, dominantly associated with C-Suite.

These are shown on a large correlation panel (A1 sheet), which is available in the Supplementary Material; this has been split into three separate figures (Figure 5A–C).

The most obvious feature of the logging is that it is extremely difficult to define a boundary between the Arroyo Diablo and Olla formations [20]. The percentage of C-Suite sandstone does increase eastwards away from the basin margin (Figure 6A), but it is not systematic, and there is an obvious “Low C” unit in the middle of the sections. It is also worth noting that the usual depiction of the Olla–Arroyo Diablo boundary shows increasing L-Suite upwards while our data show that this is not the case. The Red Mudstone association may be a better predictor of the Arroyo Diablo Formation, as there is an irregular but clear increase basinward, reflecting a strong association with the C-Suite association; again, if the boundary were defined on this, it shows the Arroyo Diablo expanding towards the basin margin (Figure 6B). Mixed units are almost unknown in the basin as a whole, but they are locally common in the transition zone (Figure 6C). With a single exception, they are restricted to the middle part of the stratigraphy shown on these sections.

The best interpretation of these results is that the transition zone is tripartite. Recalculating the data in Table 2 to give the average facies association composition of logs within the three zones (Table 3) shows:

1. A lower, C-Suite dominant unit which has a predictable basinward increase in C-Suite;
2. A middle, L-Suite dominant unit which extends relatively far into the basin and is characterised by the highest proportion of black siltstone and of mixed association and the lowest percentage of red mudstone;
3. An upper unit which is C-Suite dominant and shows a marked expansion of the C-Suite toward the basin margin.

This middle unit is shown in the Google Earth images in Figure 6. The extension of the unit into the basin is clear on Figure 6E while the nature of the thick, proximal, unit of L Suite is shown in Figure 6F. We believe that it would be almost impossible to put a meaningful boundary line between Olla and Arroyo Diablo on either map or section and that it would be better to consider all interbedded C- and L-Suite deposits as part of the Olla Formation.

4.3. Stable Minerals of Fish Creek–Vallecito Basin

It should be noted here that although the initial counts of overall heavy mineral species abundance were carried out, the data provide no significant variation for the purpose of

the study. The trends are clearer from stable mineral ratios and variational analysis. The count data are shown in two formats in the Supplementary Materials: full heavy mineral assemblages and assemblages with the calcic-amphibole removed. Calcic-amphibole is an unstable mineral that is removed quickly from an assemblage once burial diagenesis has begun, with this diagenetic effect having a dominant effect on the total heavy mineral assemblages in the FCVB [9].

The most important stable mineral ratios for distinguishing provenance in the FCVB are garnet:zircon (GZi), apatite:tourmaline (ATi), and rutile:zircon (RZi) [9]; for information on the overall heavy mineral assemblages, please refer to the Supplementary Data (Table S1). Results for stable mineral ratio pairs can be seen in Figure 7 (and Supplementary Data Table S2). Figure 7A,B illustrate all ratio pair data for the Fish Creek-Vallecito Basin stratigraphy, with the exception of those from the Olla Formation. The majority of data plot within one of two clear fields, one representing locally derived sediments (L-Suite) and one representing the Colorado River derived sediments (C-Suite). The Split Mountain Group and Lycium Member are of pre-Colorado L-suite provenance and Hueso Formation, and Canebrake Conglomerate are of syn/post-Colorado L-suite provenance; the two show little variation in the basin catchment. A point of interest beyond the Olla Formation is the Wind Caves Member. Samples from this stratigraphic level are split, most plotting in the C-suite field but a few samples plot within the L-suite field. This supports the current understanding that the Wind Caves Member represents the arrival of the Colorado River into the basin [6,8,9,20].

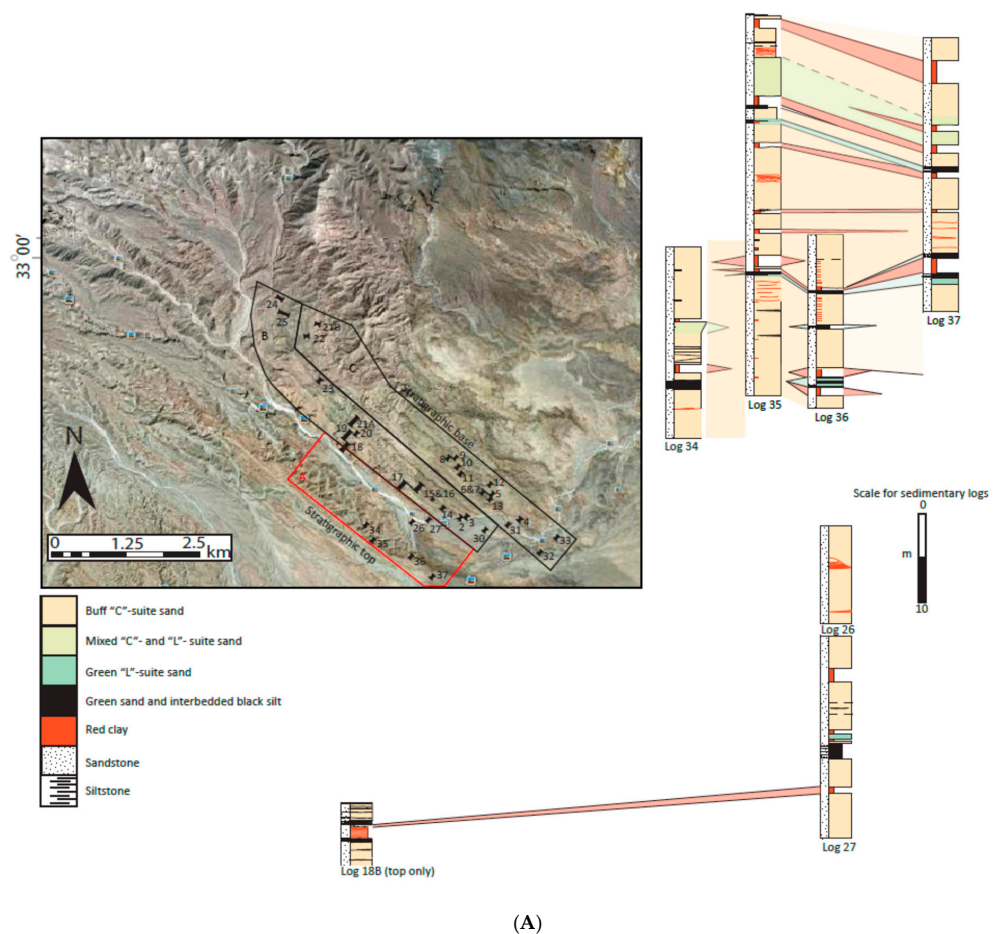


Figure 5. Cont.

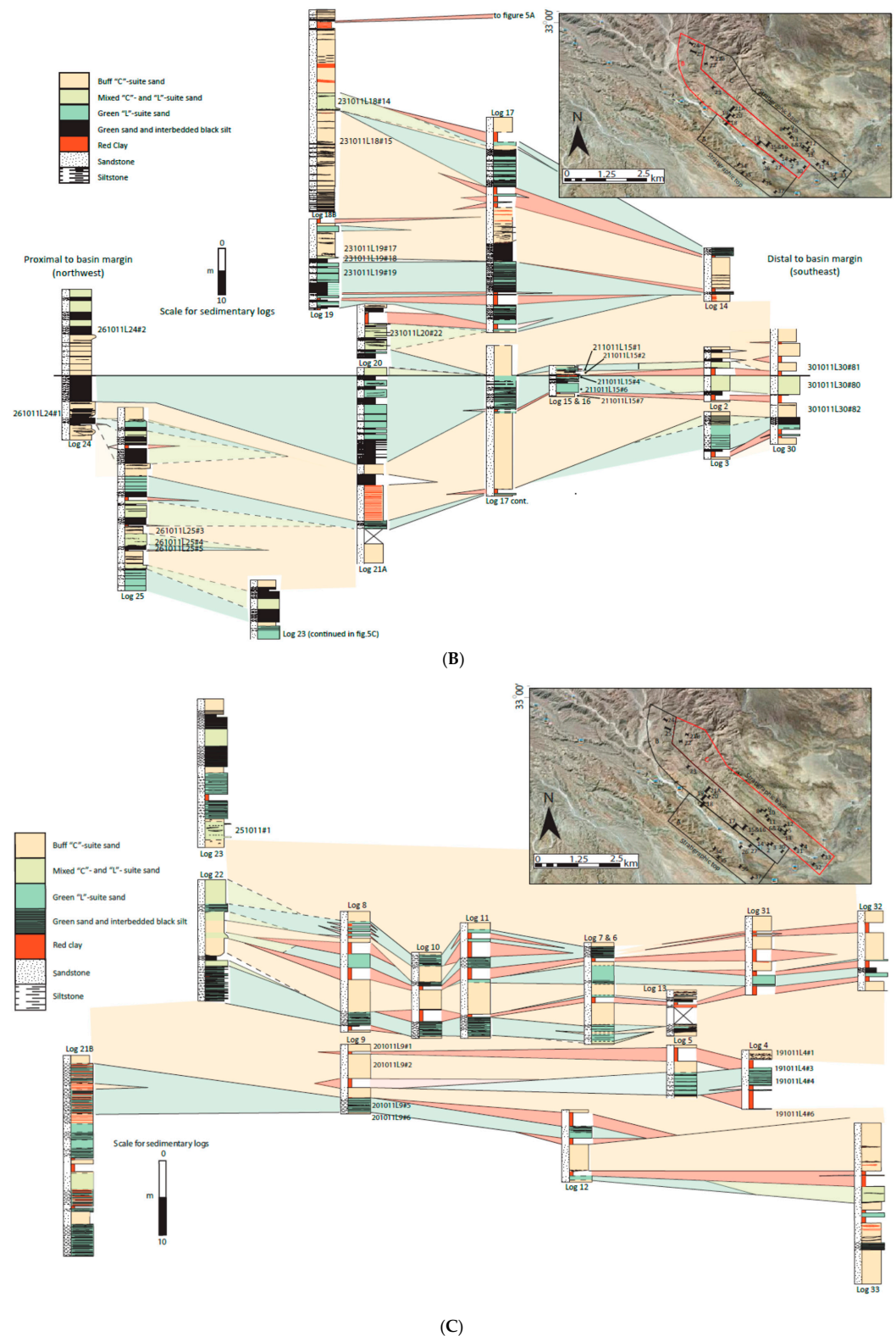


Figure 5. (A) Part one of the log correlation panel (full panel in Supplementary Data). This includes the correlation of sedimentary log columns 34, 35, 36, 37 and 27, via log 18B with **(B)**. **(B)** Part two of the log correlation panel including sedimentary log columns, 24, 25, 19, 21A, 17, 15, 16, 14, 2, 3, 30, with the continuation of 18B linking to **(A)** and 23 continuing to **(C)**. **(C)** Part three of the log correlation panel including sedimentary log columns, 21B, 22, 8, 9, 10, 11, 6, 7, 12, 13, 5, 4, 31, 32, 33 and the continuation of 23 from **(B)**.

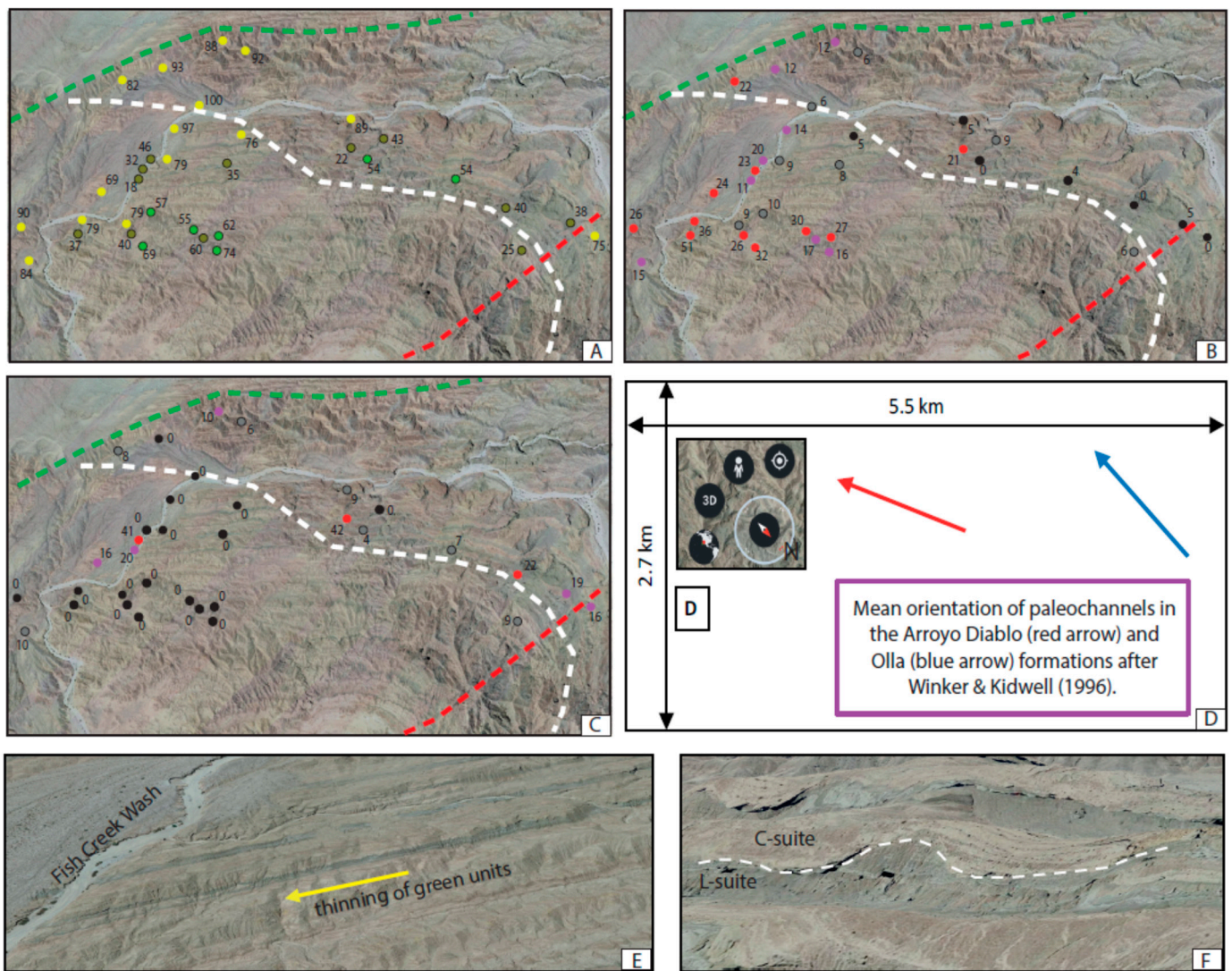


Figure 6. (A–C) are vertical Google Earth image (SSW up) to show the well-exposed part of the Olla-Diablo Transition zone in true stratigraphic orientation. In (A–C) the percentage of various facies are shown at the mid-point of each section (see Figure 3 for locations and Figure 5 for section details); on all three figures: green dashed line—top of Olla/Diablo Formation; red dashed line—axial trace of the Fish Creek Anticline; white dashed line—mapped transition zone from Dorsey et al. (2006). (A)—percentage of Colorado sand (C-Suite) as a percentage total sandstone (C + L + L & S + Mixed) in each section. Yellow highlight, >75% C-Suite; green highlight, 50–74% C-Suite; Olive highlight, <50% C-Suite.; (B)—percentage of Red Mudstone Facies in each section. Red highlight, >20% red mudstone; Pink highlight, 11–20% red mudstone; Grey highlight, 6–10% red mudstone; Black highlight 0–5% red mudstone.; (C)—percentage of Mixed Facies in each section. Red highlight, >20% mixed units; Pink highlight, 11–20% mixed; Grey highlight, 6–10% mixed; Black highlight 0–5% mixed.; (D)—Scale and orientation (compass symbol) of (A–C) and palaeocurrent directions oriented to these figures (after Winker and Kidwell, 1996).; (E)—Tilt Google Earth image of the eastern (distal) end of the middle, L-Suite unit; View SW; Fish Creek Wash to the left of the picture. Note the continuity of units and the subtle thinning of the green units to the left (SE, basinward).; (F)—Tilt Google Earth image of the western (proximal) end of the middle, L-Suite unit; View SW. Note the C-Suite channels cutting into thick L-Suite units. Note the accretion surfaces in the lower channelised unit and the leftward stepping (basinward) of the succeeding channel.

Table 3. Summary data for the three sections (Upper, Middle, and Lower) identified within the Olla/Diablo transition zone. Note that Section 18 has been left out as it crosses the mapped boundaries between the Middle and Upper units.

Unit	Sections Included	Percentages of Each Facies by Section					C Suite as a % Total Sand	
		Buff sst (C Suite)	Green sst (L Suite)	Green sst & Silt (L)	Mixed (L & C)	Silts-tone		Red Mudstone
Upper	14, 17, 26, 27, 34, 35, 36, 37	74.9	2.1	4.9	4.2	2.6	11.4	87
Middle	1, 2, 3, 15/16, 19, 20, 21A, 21B, 22, 23, 24, 25, 30	33.9	15	13.1	12.2	16.5	9.3	46
Lower	4, 5, 6/7, 8, 9, 10, 11, 12, 13, 31, 32, 33	49	8.7	13.3	1.5	3.6	23.9	68

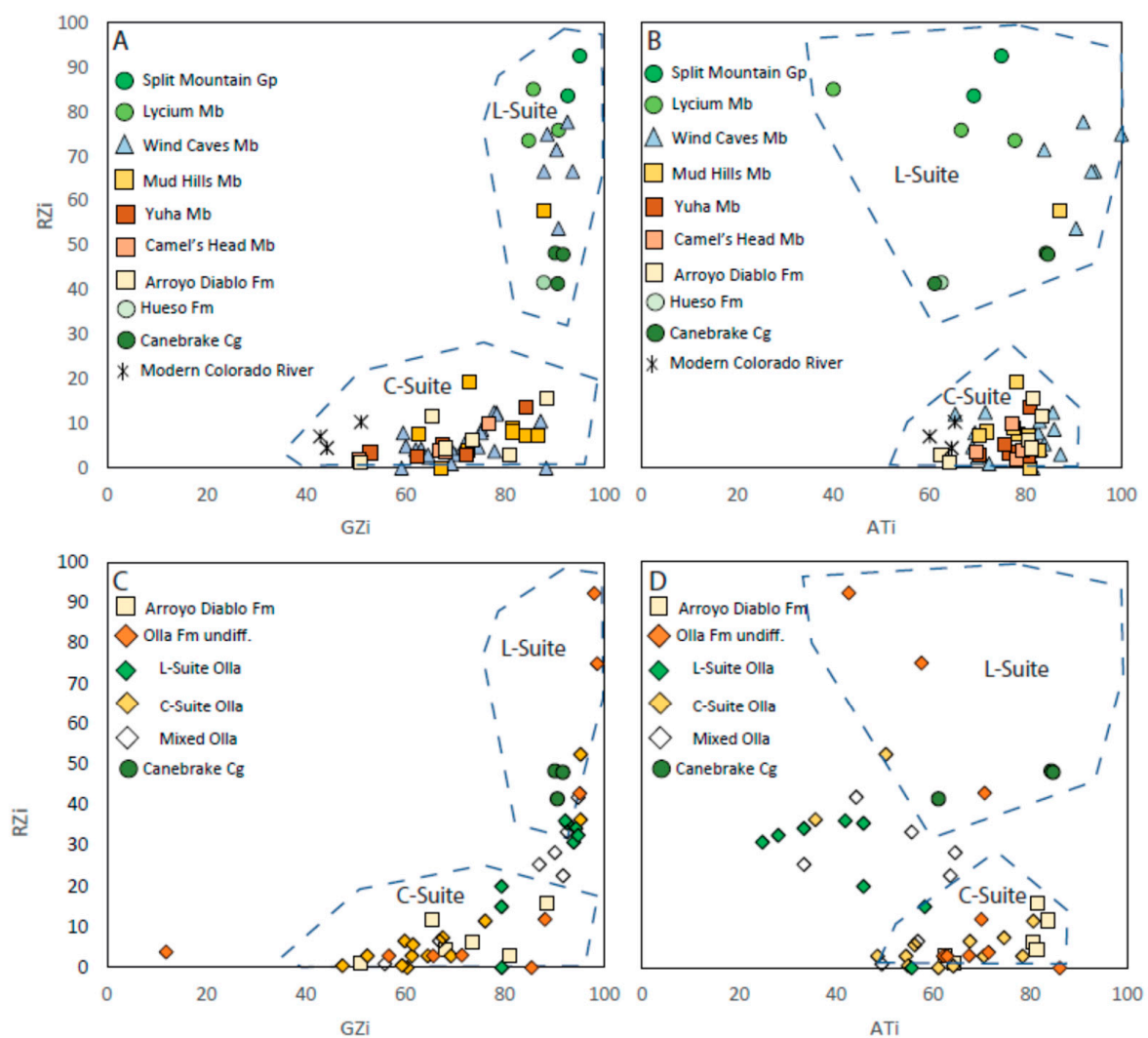


Figure 7. (A) GZi vs RZi crossplot including all data points, excluding the Olla Formation. (B) ATi vs RZi crossplot including all data points, excluding the Olla Formation. (C,D) show the GZi vs RZi crossplot and the ATi vs RZi crossplot with the Olla Formation samples separated into L-suite, C-suite, mixed and undifferentiated. A C-suite sample set (Arroyo Diablo) and an L-suite sample set (Canebrake) remain for comparison.

The Olla Formation samples were omitted from Figure 7A,B due to it being derived from a combination of C-suite and L-suite sediments. The omission provides a clear view of the two provenance fields. Figure 7C,D illustrate an uncluttered view of samples from

the Olla Formation. Some Olla Formation samples plot in the L-Suite field and some in the C-Suite field while many plot in an intermediate position between the two fields. The distinction between the two source fields is very clear. L-Suite samples have a much higher RZi compared to the C-Suite deposits. The two groups have similar ranges of ATi, but the C-Suite sediments (including the modern Colorado River) generally have a lower GZi.

To better understand the Olla Formation samples on these plots, they are labelled based on field observations (Figure 7C,D). Olla samples have been separated into the buff yellow C-suite sands, green L-suite sands, and lighter green sand that is interpreted, from field observations alone, to be a mixture of the two end members. In addition, there are undifferentiated Olla samples that sit within both fields.

Figure 7C shows that the C-Suite Olla Formation samples have very low RZi and moderate-high GZi, typical of C-Suite sediment (Arroyo Diablo Formation remains for comparison). In addition, two L-Suite samples sit in this field. However, L-Suite samples do not sit in the L-Suite Field, but they tend to have a lower RZi, much the same as the 'mixed' Olla Formation samples. The RZi is not usually so low as to put them in the C-Suite field but falls somewhere in between. This may indicate that even in the L-suite, green Olla sand has some degree of mixing with the Colorado derived sediment. Figure 7D, on first look, appears to show some discrepancy, with all samples (Figure 7B included) having a moderate to high ATi, with RZi being the differentiating factor between the two provenance fields. The exception is that most L-suite samples and some mixed suite samples have a notably lower ATi, which could be an environmental indicator related to flood plain storage duration or sediment recycling rather than representing a change in provenance.

4.4. Garnet Geochemistry

The garnet geochemistry data allow the comparison of geochemical compositions of garnets within the Olla Formation. The modern Colorado River, upper Wind Caves Member, Camel's Head Member, and Arroyo Diablo Formation provide a garnet geochemical signature of a purely C-Suite sediment, and the Canebrake Conglomerate and the L-suite lower Wind Caves Member provide an L-Suite sediment garnet signature. Three samples were taken from the Olla Formation from the buff, C-Suite Olla Formation, the L-Suite green sands, and the intermediate pale green sands, respectively. The data can be seen in Figure 8 (raw data available in Supplementary Data Table S3).

The garnet geochemistry profile of the L-Suite Canebrake Conglomerate is dominated by Type Bi and Type Bii garnets with some Type D garnets and a single Type A garnet grain. The C-Suite Arroyo Diablo garnet geochemistry profile is dominated by Type Bi garnets with secondary Type A garnets and a minor quantity of Type Bii, Type Ci, and Type D garnets. The C-Suite Olla sample has a garnet geochemistry profile almost identical to that of the Arroyo Diablo Formation with a dominance of Type Bi garnets and secondary Type A garnets and a few grains each of Type Bi garnets (some of which are very close to being Type Ci garnets) and Type D garnets. The L-Suite Olla sample is dominated by Type Bi garnets with some Type Bii and D garnets, similar to the Canebrake Conglomerate, but the clearest difference compared to C-suite samples is the absence of Type A garnet in the L-suite sediment. The mixed Olla Formation sample is comparable with the L-Suite samples with a few grains of Type A garnets and fewer Type Bii garnets.

This new data supports the garnet geochemistry work from Nicholson et al. [9], which shows an L-Suite sample from the Wind Caves Member, pre-Colorado River, which is dominated by Type Bi and Bii garnets and shows the similar absence of Type A garnets. The Wind Caves Member after arrival of the Colorado River then contain less Type Bii garnets and slightly more Type D garnets but most notably input of Type A garnets and minor quantities of Type Ci garnets. This is the same for the Camel's Head Member and the Arroyo Diablo Formation, as well as modern Colorado River samples.

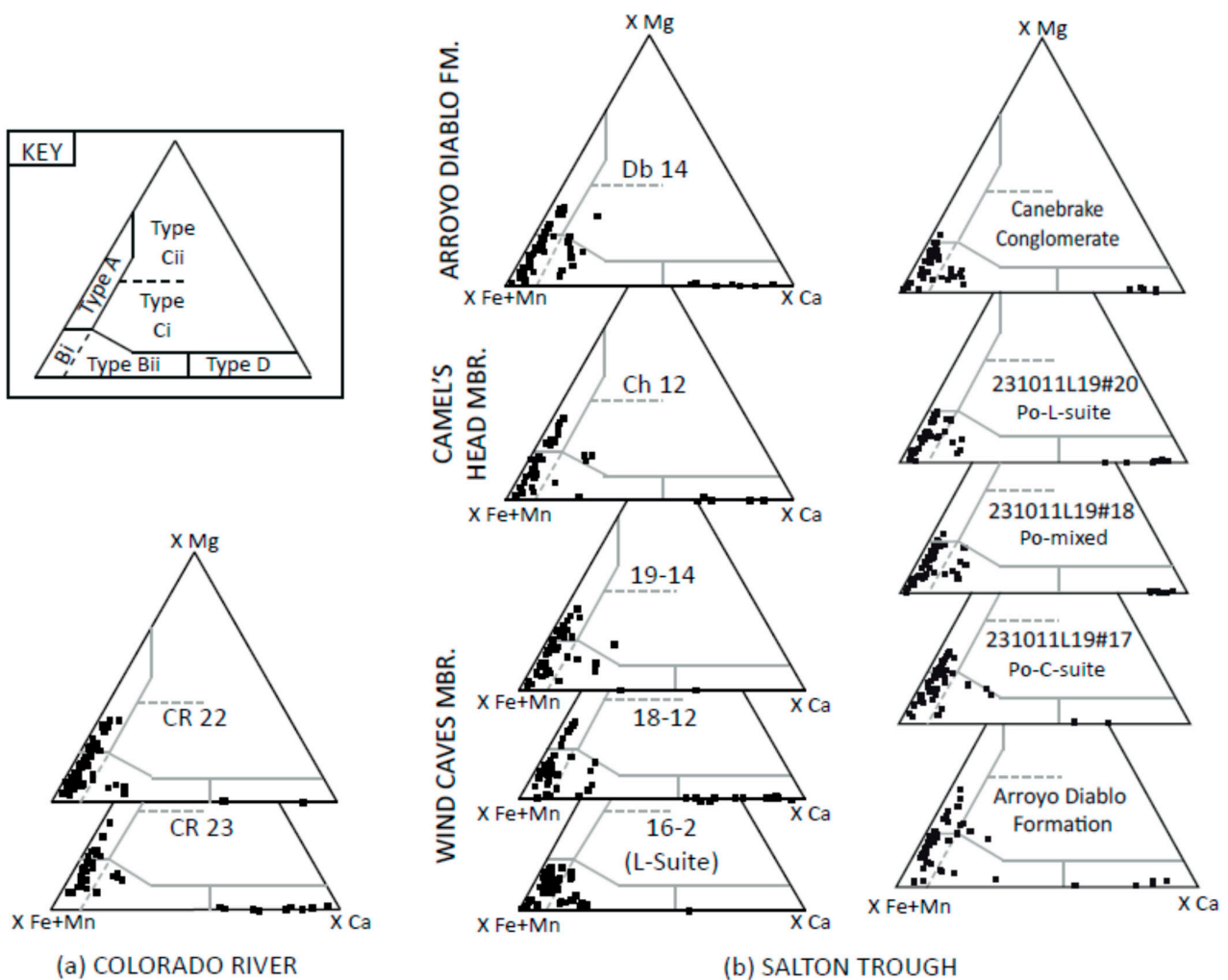


Figure 8. Garnet geochemistry ternary diagrams showing data from Nicholson ([9]; samples) and additional plots for this study. Ternary diagram based on compositional fields of garnets, used to plot garnet geochemistry, from Mange and Morton [48]. Type A—high Mg, low Ca. High-grade granulite metasedimentary rocks and charnockites. Sometimes intermediate-silicic deep crustal igneous rocks. Type B—low-Mg, low Ca, often rich in Mn. Intermediate-acidic amphibolites facies igneous rocks. Type Bi— $X_{Ca} < 10\%$ —granitoids, Mn-rich. Type Bii— $X_{Ca} > 10\%$ Type C—high-Mg, high-Ca. high-grade mafic and ultramafic gneisses. Type Ci— $X_{Mg} < 40\%$ Metabasic rocks. Type Cii— $X_{Mg} > 40\%$ ultramafic rocks eg. pyroxenites and peridotites Type D—abundant Fe^{3+} -Ca. contact or thermally metamorphosed calcareous sediments, ultra-high temperature calc-silicate granulites. If a clinopyroxene dominated assemblage, garnets are from low-grade metabasic rocks.

4.5. Detrital Zircon U-Pb Dating

Detrital zircon U-Pg age spectra are shown in Figure 9 and described below, with raw data available in Supplementary Data Table S4. The zircon age profile for a C-suite sediment was taken from the Camel's Head Member (Figure 9a) and shows a wide variety of zircon ages. There is a broad range of grains 0–200 Ma with another at 300–400 Ma. There are also zircon grains dating between 1–2 Ga with peaks from 1.1–1.2 Ga, 1.4–1.5 Ga, and 1.7 Ga, with additional peaks at 2.1 Ga, 2.4 Ga, and 2.8–2.9 Ga. By contrast, the L-Suite end member, taken from the Canebrake Formation (Figure 9b), is dominated by zircons of 90–200 Ma with a small subsidiary peak at about 1.7 Ga. This is a significantly narrower age range than the sediment coming from the Colorado River. These end members are consistent with Colorado-derived and locally-derived zircon age spectra from Nicholson et al. [9] and Kimbrough et al. [7].

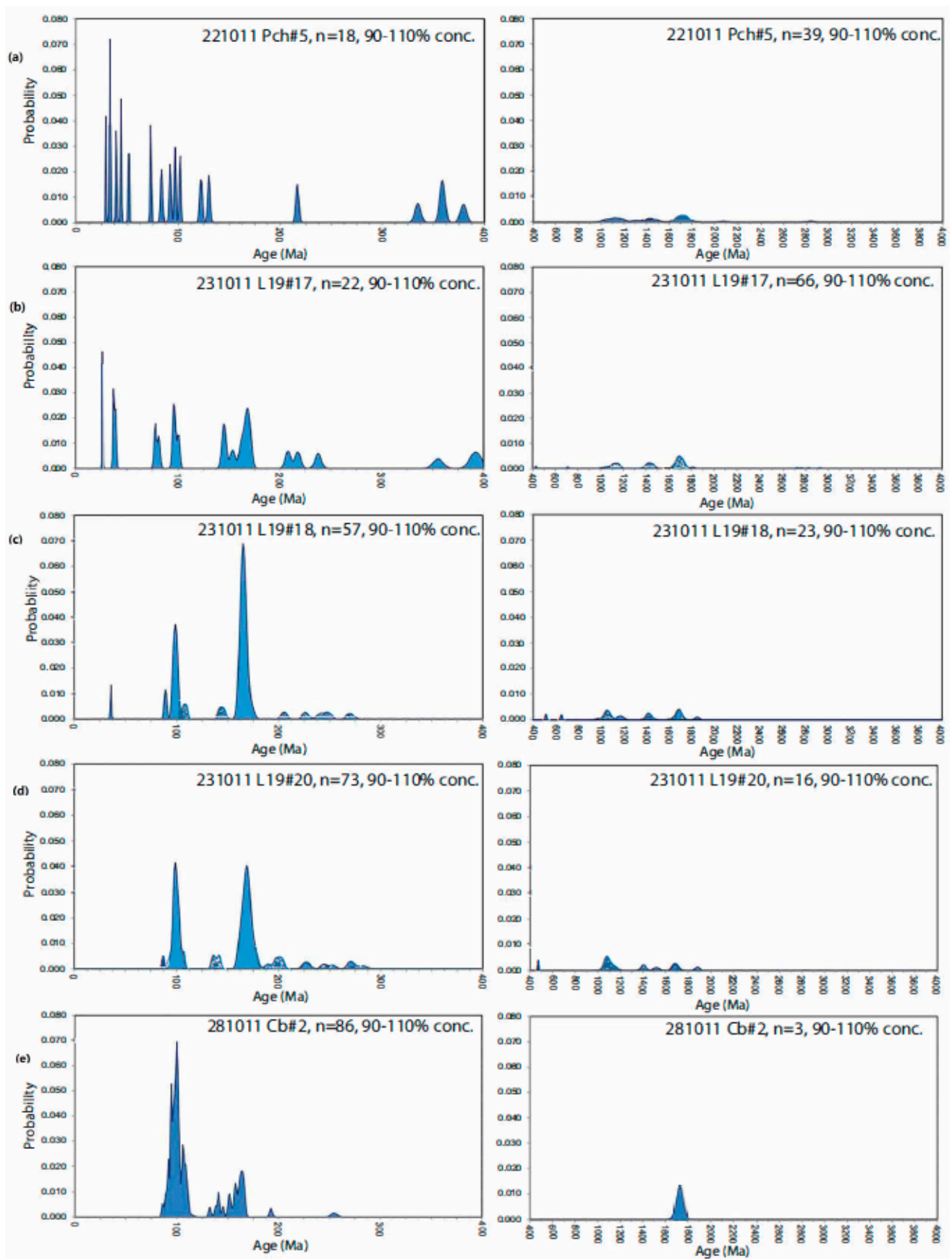


Figure 9. (a–e) Detrital Zircon U-Pb Age spectra for three Olla samples, a locally derived Canebrake sample and a Colorado derived Camel’s Head sample.

Samples from the Olla Formation represent buff, C-suite Olla (Figure 9c), intermediate, mixed Olla (Figure 9d), and green L-suite Olla (Figure 9e). As expected, the C-suite Olla sample shows a very similar zircon age profile to that of the Camel's Head Member. Both the intermediate and L-suite Olla samples show some younger peaks (0–100 Ma) seen in the C-suite samples, although this is much less obvious for the L-suite buff sample. They also both show some older zircon grains with ages of >1 Ga; however, these peaks are much less prominent compared to the C-suite samples. It should be noted that even the L-suite Olla sample appears to contain zircons that have a Colorado source. To better understand this, Figure 10 shows the data in a percentage mixing plot. This illustrates that the green L-suite Olla sample contains around 20% Colorado-derived zircon grains and that the mixed Olla sample (#18) contains around 30% contribution from the Colorado River. The locally sourced Canebrake Conglomerate provides a sample showing the most locally derived zircon signature, which can also be seen in the work of Cloos et al. [57], Nicholson et al. [9], and Kimbrough et al. [7].

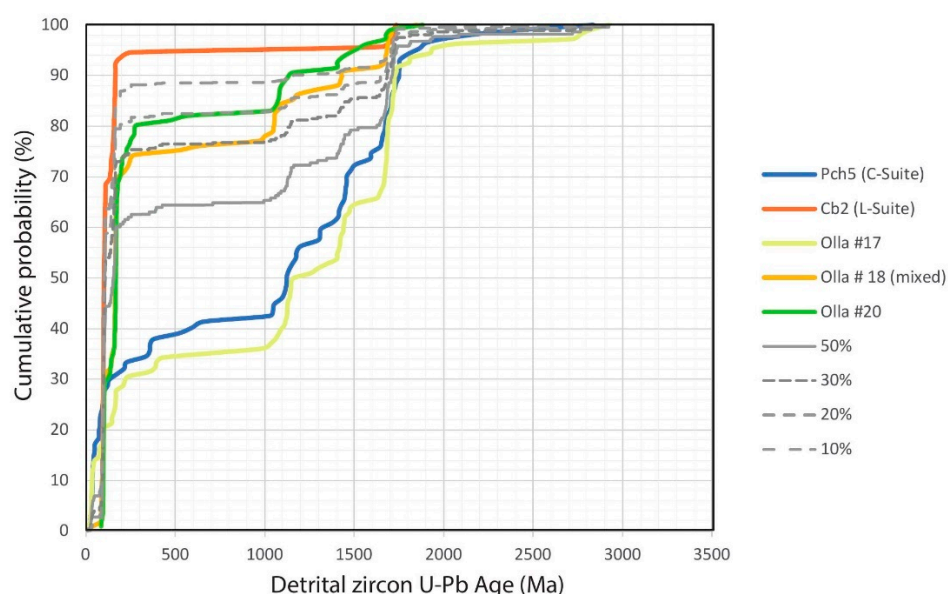


Figure 10. Cumulative probability plot of detrital zircon ages from the Palm Springs Group and Camel's Head Member. The grey lines represent mixing of detrital zircons populations of C Suite (Olla #17) and L Suite (Cb2). All Olla samples show some degree of mixing, even those assumed *a priori* to be purely L Suite (e.g., Olla 20).

5. Discussion

5.1. Provenance of Large Rivers

The Colorado is one of the 30 largest rivers on Earth, measured both by catchment and length [58], so its behaviour and evolution are globally significant. Of these 30 rivers, only three cross a strike-slip plate boundary and deposit at least part of their delta in an active tectonic zone: Amur [14], Orinoco [12], and Colorado [8]. Two other large rivers also form at active collisional margins, constrained by the resulting topography. Sedimentation from the Ganges-Brahmaputra system is pinned by the collisional orogen of the Burma Arc, and part of its sediment load ends up in the Sunda Trench [59]. The Tigris-Euphrates is relatively young (Pliocene-Holocene), and the river and delta have changed significantly because of rapid foreland subsidence, high rates of sediment supply, and local base-level changes in the Persian Gulf [60]. All of the other great rivers deliver their sediment load to passive margins, so the Colorado is one of the few great rivers on Earth that has a delta that is controlled by tectonic processes other than post-rift subsidence. This suggests that any investigation of the palaeo-delta of the Colorado must honour the tectonic setting and explain how depositional processes were influenced.

The Colorado, Amur, and Orinoco share another characteristic: they each deposit distinctive sands that can be clearly distinguished from locally derived material [9,23,61]. It has always been a matter of research and debate how tributaries influence the bed load of large rivers. Van Andel [22], in his classic study of the heavy minerals of the Rhine, pointed out that “... *The influence of a tributary is not determined by its drainage area, but by the original size of the heavy minerals and by the heavy mineral content of its sediments. On the whole the changes resulting from supply by affluents are small and of limited extent.*” In this case, although there was a large influx of volcanic hornblende and other related heavy minerals into the middle Rhine, these declined in importance downstream—possibly due to their labile nature. In their study of the Amur catchment, Nicholson et al. [23] found that the sands deposited in the palaeo-delta on Sakhalin were clearly sourced from the Zeya-Bureya Basin, 2000 km upstream; tributaries had little or no influence. It would appear that provenance mixing in major rivers is rare, except in the headwaters. This is partly due to the scale of the major river compared to tributaries [22]; in the case of the Amur, the modern river system aggrades above the present level of the flood plain, meaning that tributaries enter through lakes, bringing no bedload to the main trunk river (personal communication from Professor A.P. Sorokin, 2001). In the extreme example, the Cross River flows across the Niger delta, completely independent of the main stream [62], so there is no signature of the volcanic rocks of the Cameroon Highlands in the Niger Delta [63]. This focuses attention on the mixed provenance of the Olla Formation, which would appear to be unusual.

Such distinctive provenance can be long-lived. In the case of the Colorado deposition in the FCVB, the main river provenance persisted from about 5 Ma until the end of Colorado sedimentation at 2.5 Ma. This interval of unchanged provenance is brief compared to other systems: the Amur has had broadly unchanged provenance for about 23 Ma (21 Ma recorded in the receiving basin on Sakhalin [14]); the Nile has about 30 Ma of near-identical provenance since near the start of the Oligocene (about 30 Ma [64]); and the Mississippi has tapped into the same Appalachian and Rocky Mountain sources since at least the start of the Cenozoic (up to 65 Ma [65]).

The Colorado belongs to a group of rivers (Amu Darya, Colorado, Euphrates, Nile, Orange, Indus, Niger, and Río Negro), which derive at least 90% of their discharge from mountain areas, yet much of their transport and deposition is through arid or semi-arid lowlands [66]. In its present configuration, it has a greatly reduced discharge and sediment flux due to the effect of upstream dams [67]. In the case of the Colorado, the tectonics and climate of the entire catchment and its antecedents are also important factors to consider.

5.2. External Forcing Factors

The results presented here suggests that the distal margin of the Olla Formation (Figure 6; Table 3) records changes in the balance between local and Colorado sediment derivation in the FCVB. Our middle unit of the Olla Formation transition zone seems to represent a retreat of the Colorado River from the basin margin and an advance of locally derived sedimentation. This is unlikely to be a major tectonic factor as the Colorado Plateau was already elevated [68]; the Colorado River was already well established [20]; and the Elsinore Fault was not initiated until 1.6 million years later [16].

The Pliocene climate of the western US was warmer than the present day with a dominance of winter rainfall and a general drying and cooling trend through the Pliocene [69]. The Olla Formation was deposited towards the end of the mid-Pliocene Warm Period (mPWP, [69]) when surface temperatures were still higher than today, although modelling suggests that the Colorado Plateau may have experienced sub-zero temperatures [70]. Astronomical forcing (Milankovitch cyclicity) has been modelled in detail through the Mesozoic and Cenozoic [71], and there is a strong correlation with the climate as reflected in $\delta^{18}\text{O}$ records from the Pliocene, which vary in both 41 Ka and 100 Ka cycles [70,72,73]. This would have influenced rainfall and temperatures but does not appear to have significantly affected Colorado River sedimentation. This conclusion is supported by the work of Galloway et al. [74], who studied the history of sedimentation in the Gulf of Mexico and

concluded that the Pliocene sediment yield from the eastern part of the Rocky Mountains and Colorado Plateau were fairly constant through the Pliocene, if not longer [75].

Climate may, however, have had an effect on the amount of local sedimentation, which would have been more sensitive to local rainfall variation than the very large, buffered, Colorado system. The middle L-Suite unit is 130–145 m thick; assuming that the 2520 m of the Olla Formation was deposited at a constant rate, this implies that the middle unit was deposited in 72,000–81,000 years, which is in the Milankovitch range.

5.3. Provenance Mixing—Controls and Processes

The provenance of the Colorado has been unchanged for about 2.5 Ma, so the tectonic evolution of the catchment cannot be a factor: the sediment source has remained the Colorado Plateau throughout this period [8]; this is supported by the compilation and modelling work of Fernandes et al. [68], which shows that the Colorado Plateau has been elevated since the Paleocene. However, in their study of the Sylhet River, Sincavage et al. [76] pointed out that there is a distinction between tectonic scale (10^2 km) and event scale (10^1 km) processes; they demonstrated that although tectonics created steeper and more favourable pathways into the receiving basin, the Sylhet continued to occupy a longer and less steep existing channel which had been enhanced by large flood events. Their dictum that large-scale stochastic events should have equal weight to tectonic and climatic events—in the case of the Sylhet, in the creation of pre-existing topography—is clearly applicable to the Olla Formation. To put it at its simplest, the Olla would not exist without local topography capable of generating sediment load for local rivers, which would be tributaries of the Colorado.

The question then becomes: how did the mixing occur? All authors agree that the Olla is laterally equivalent to and intermediate between the Canebrake and Arroyo Diablo formations [9,16,20,32]. It is clear (Figures 5 and 6) that the mixed provenance of the Olla is not uniform—rather, it is interbedding of material from two sources, which retain a distinct facies identity and composition. However, stable heavy mineral ratios, garnet geochemistry and U-Pb detrital zircon dating show that there are some true mixed units, which tend to be restricted to the middle unit of the Olla (Figure 6), so the process of mixing must be localised within the basin. There are three facts that must be taken into account. First, the sedimentological analysis of Winker [20] suggests that Olla L-Suite units appear to have been deposited in shallower, faster-flowing streams than the C-Suite facies. Second, L-Suite rocks have palaeocurrent directions that are slightly oblique to the trends in C-Suite [6] (see Figure 6D). Third, post-Colorado lacustrine deposits of the Tapiado Formation do not overlap with the Olla outcrop (Dorsey et al. [16]—their Figure 3).

The heavy mineral assemblages of the L-suite and C-suite are very similar with no obvious variations. As shown previously by Nicholson et al. [9], the stable mineral pairs, however (Figure 7), do show the differences between C-suite and L-suite sediment, with data from the entire stratigraphic section providing very clear C- and L-suite fields. In the majority of the buff, C-suite Olla samples sit within the C-suite compositional field [9], and some L-suite samples sit within the L-suite field, but many are on the periphery, indicating the possibility of a mixed provenance. This suggests that although the green sediment of the Olla Formation is referred to as L-suite, there is a degree of mixing with C-suite sediments. The presence of Type A garnets is also diagnostic of C-suite sediments and the absence of this garnet type marks an L-suite sediment, but in the Olla Formation, a few grains of Type A garnets can be found in the mixed units. In some cases, there are just a few grains of Type A or Ci grains, and so there is some limitation to the certainty. It is the combined use with other datasets that increases the certainty. Increasing the sample size of garnet grains tested would help to increase the trend certainty of the garnet data.

Trends seen in the stable mineral ratios and garnet geochemistry data, further confirmed by mixing plots of detrital zircon ages (Figure 10), show that the L-Suite Olla Formation sample is still a hybrid of local (80%) and Colorado-derived (20%) sediment. This suggests that there were compositionally distinct, locally derived fluvial channels on

the palaeo-Colorado floodplain but that these channels incorporated some material as they cannibalised older Colorado River-derived deposits on the floodplain.

6. Conclusions

The combination of review, field, and laboratory work detailed in this paper leads to five important conclusions:

1. The Pliocene Colorado River system was unusual among the Earth's great rivers in having its delta deposited in a strike-slip plate boundary and in having a floodplain depositional unit (Olla Formation) with a genuine mixed and interbedded provenance;
2. The interbedding and mixing of far-travelled and locally derived deposits was facilitated by persistent local topography within and adjacent to the receiving basin;
3. Climate, tectonics, and overall geometry of the sediment routing system of the Colorado River remained relatively constant through the deposition of the Olla and Arroyo Diablo formations. However, climate variation on the Milankovitch scale may have had an effect on the local sediment flux, which would have been more sensitive to local rainfall variation than the very large, buffered, Colorado system;
4. The low ATi of much of the Olla Formation, when compared to the L- and C-suite end-member samples, could be the result of longer time spent in storage on the flood plain top environment prior to burial. It should also be acknowledged that the lower ATi could be the result of sediment recycling along the lower Colorado River corridor as a result of remobilization from fill-and-spill processes upstream of the FCVB [77–80];
5. The combination of stratigraphic, sedimentological, and heavy mineral work suggests that the Olla L-Suite was deposited on the distal part of the Canebrake alluvial fan system still with a depositional slope towards the basin. Deposition of the Olla was probably by both the main trunk stream of the Colorado and smaller tributaries coming across the fans. The migration of the main river could have cannibalised fan toe deposits, and vice versa, leading to true mixed provenance units in a restricted area.

Although this study focuses on a small part of a medium-sized basin, it illustrates the importance of local factors in determining the sedimentary record of one of the Earth's great rivers.

Supplementary Materials: The following are available online at <https://www.mdpi.com/article/10.3390/geosciences13020045/s1>, Table S1: Basic heavy mineral count data., Table S2: Stable heavy mineral ratio data., Table S3: Garnet Geochemistry data (3A: 231011 L19#17., 3B: 231011 L19#18., 3C: 231011 L19#20., 3D: 301011 Pd1)., Table S4: U-Pb detrital zircon data (4A: 221011 Pch#5., 4B: 281011 Cb#2., 4C: 231011 L19#17., 4D: 231011 L19#18., 4E: 231011 L19 #20). Figure S1: Sedimentary log correlation panel.

Author Contributions: Author contributions are as follows; conceptualization, P.M. and D.M.; methodology, P.M.; validation, D.M., P.M., U.N and D.F.; formal analysis, P.M.; investigation, P.M.; resources, P.M., U.N., D.M and D.F.; data curation, P.M. and U.N; writing—original draft preparation, P.M.; writing—review and editing, D.M., and U.N; supervision, D.M.; project administration, P.M.; funding acquisition, P.M., D.M. and U.N. All authors have read and agreed to the published version of the manuscript.

Funding: P.M. was supported by a Siddall Scholarship through the University of Aberdeen; U.N. was supported by a NERC CASE Award with Sakhalin Energy Investment Company as the industrial partner. Fieldwork in California was supported in part by the ASTARTE Consortium, led by D.M. at the University of Aberdeen.

Data Availability Statement: All new raw data is made available in the supplementary files linked with this manuscript.

Acknowledgments: We would like to thank Ray Ingersoll for introducing DM to the area and Rachel Flecker for her role in helping initiate this project. Above all we owe a huge debt of gratitude to Andrew Morton for his encouragement and assistance in producing this work. We thank Keith Howard and four anonymous reviewers for their careful reviews and helpful comments.

Conflicts of Interest: The authors declare no conflict of interest. The funders had no role in the design of the study; in the collection, analyses, or interpretation of data; in the writing of the manuscript, or in the decision to publish the results.

References

1. Axen, G.J.; Fletcher, J.M. Late Miocene–Pleistocene extensional faulting, northern Gulf of California, Mexico and Salton Trough, California. *Int. Geol. Rev.* **1998**, *40*, 217–244. [[CrossRef](#)]
2. Winker, C.D.; Kidwell, S.M. Paleocurrent evidence for lateral displacement of the Pliocene Colorado River delta by the San Andreas fault system, southeastern California. *Geology* **1986**, *14*, 788–791. [[CrossRef](#)]
3. Dibblee, T.W., Jr. Geology of the Imperial Valley Region, California. *Geol. South. Calif. Calif. Div. Mines Geol. Bull.* **1954**, *70*, 21–28.
4. Dibblee, T.W. Stratigraphy and Tectonics of the San Felipe Hills, Borrego Badlands, Superstition Hills, and Vicinity. In *The Imperial Basin – Tectonics, Sedimentation and Thermal Aspects*; Rigsby, C.A., Ed.; Pacific Section Society of Economic Paleontologists and Mineralogists: Los Angeles, CA, USA, 1984; Volume 40, pp. 31–44.
5. Dibblee, T.W.; Ehrenspeck, H.E. Field Relations of Miocene Volcanic and Sedimentary Rocks of the Western Santa Monica Mountains, California. In *Depositional and Volcanic Environments of Middle Tertiary Rocks in the Santa Mountains, Southern California*; Weigand, P.W., Fritsche, A.E., Davis, G.E., Eds.; Pacific Section Society of Economic Paleontology Mineralogy: Los Angeles, CA, USA, 1993; Volume 72, pp. 75–92.
6. Winker, C.D.; Kidwell, S.M. Stratigraphy of a marine rift basin: Neogene of the Western Salton Trough, California. In *Field Conference Guide 1996*; Patrick, L., Abbott, J.D., Eds.; Pacific Section American Association Petroleum Geology: San Diego, CA, USA; Volume 73, pp. 295–336.
7. Kimbrough, D.L.; Grove, M.; Gehrels, G.E.; Dorsey, R.J.; Howard, K.A.; Lovera, O.; Aslan, A.; House, P.K.; Pearthree, P.A. Detrital zircon U–Pb provenance of the Colorado River: A 5 m.y. record of incision into cover strata overlying the Colorado Plateau and adjacent regions. *Geosphere* **2015**, *11*, 1719–1748. [[CrossRef](#)]
8. Dorsey, R.J.; Housen, B.A.; Janecke, S.U.; Fanning, C.M.; Spears, A.L.F. Stratigraphic record of basin development within the San Andreas fault system: Late Cenozoic Fish Creek–Vallecito basin, southern California. *Geol. Soc. Am. Bull.* **2011**, *123*, 771–793. [[CrossRef](#)]
9. Nicholson, U.; Carter, A.; Robinson, P.J.; Macdonald, D.I.M. Eocene–Recent Drainage Evolution of the Colorado River and Its Precursor: An Integrated Provenance Perspective from SW California. In *River to Reservoir: Geoscience to Engineering*; Special Publication; Corbett, P.W.M., Owen, A., Hartley, A.J., Pla-Pueyo, S., Barreto, D., Hackney, C., Kape, S.J., Eds.; Geological Society: London, UK, 2019; Volume 488, pp. 47–72. [[CrossRef](#)]
10. Dickinson, W.R.; Beard, L.S.; Brakenridge, R.; Erjavec, J.L.; Ferguson, R.C.; Inman, K.F.; Knepp, R.A.; Lindberg, F.A.; Ryberg, P.T. Provenance of North American Phanerozoic sandstones in relation to tectonic setting. *GSA Bull.* **1983**, *94*, 222–235. [[CrossRef](#)]
11. Jefferson, G.; Lindsay, L. *Fossil Treasures of the Anza Borrego Desert*; Sunbelt Publications: Chula Vista, CA, USA, 2006.
12. Wood, L.J. Chronostratigraphy and tectonostratigraphy of the Columbus Basin, Eastern Offshore Trinidad. *Bull. Am. Assoc. Pet. Geol.* **2000**, *84*, 1905–1928.
13. Nicholson, U.; Vanlaningham, S.; Macdonald, D.I.M. Quaternary landscape evolution over a strike-slip plate boundary: Drainage network response to incipient orogenesis in Sakhalin, Russian far east. *Geosphere* **2013**, *9*, 588–601. [[CrossRef](#)]
14. Nicholson, U.; Van Der, E.S.B.; Clift, P.D.; Flecker, R.; Macdonald, D.I.M. The sedimentary and tectonic evolution of the Amur River and North Sakhalin Basin: New evidence from seismic stratigraphy and Neogene–Recent sediment budgets. *Basin Res.* **2016**, *28*, 273–297. [[CrossRef](#)]
15. Dorsey, R.J. Sedimentation and crustal recycling along an active oblique-rift margin: Salton Trough and northern Gulf of California. *Geology* **2010**, *38*, 443–446. [[CrossRef](#)]
16. Dorsey, R.J.; Axen, G.J.; Peryam, T.C.; Kairouz, M.E. Initiation of the Southern Elsinore Fault at ~1.2 Ma: Evidence from the Fish Creek–Vallecito Basin, southern California. *Tectonics* **2012**, *31*, 21. [[CrossRef](#)]
17. Crow, R.S.; Schwing, J.; Karlstrom, K.E.; Heizler, M.; Pearthree, P.A.; House, P.K.; Dulin, S.; Janecke, S.U.; Stelten, M.; Crossey, L.J. Redefining the age of the lower Colorado River, southwestern United States. *Geology* **2021**, *49*, 635–640. [[CrossRef](#)]
18. Dorsey, R.J.; Axen, G.J.; Grove, M.J.; Housen, B.A.; Jefferson, G.; McDougall, K.; Murray, L.; Oskin, M.E.; Peryam Van Wijk, J.W.; Young, E.K. Redefining the age of the lower Colorado River, southwestern United States: Comment. *Geology* **2021**, *49*, e531. [[CrossRef](#)]
19. Crow, R.S.; Schwing, J.; Karlstrom, K.E.; Heizler, M.; Pearthree, P.A.; House, P.K.; Dulin, S.; Janecke, S.U.; Stelten, M.; Crossey, L.J. Redefining the age of the lower Colorado River, southwestern United States: REPLY. *Geology* **2021**, *49*, e532–e533. [[CrossRef](#)]
20. Winker, C.D. Neogene Stratigraphy of the Fish Creek–Vallecito Section, Southern California: Implications for Early History of the Northern Gulf of California and the Colorado Delta. Ph.D. Thesis, University of Arizona, Tucson, AZ, USA, 1987; p. 494. Available online: <http://hdl.handle.net/10150/191123> (accessed on 3 July 2022).
21. Allen, P.A.; Allen, J.R. *Basin Analysis: Principles and Application to Petroleum Play Assessment*, 3rd ed.; Wiley-Blackwell: Hoboken, NJ, USA, 2013; p. 602.
22. Van Andel, T.H. *Provenance, Transport and Deposition of Rhine Sediments: A Heavy Mineral Study on River Sands from the Drainage Area of the Rhine*; Veenman: Groningen, The Netherlands, 1950.

23. Nicholson, U.; Poynter, S.; Clift, P.D.; Macdonald, D.I.M. Tying Catchment to Basin in a Giant Sediment Routing System: A Source-to-Sink Study of the Neogene—Recent Amur River and Its Delta in the North Sakhalin Basin. In *Sediment Provenance Studies in Hydrocarbon Exploration and Production*; Special Publications; Scott, R.A., Smyth, H.R., Morton, A.C., Richardson, N., Eds.; Geological Society: London, UK, 2014; Volume 386, pp. 163–193.
24. Dorsey, R.J. Stratigraphy, Tectonics, and Basin Evolution in the Anza-Borrego Desert Region. In *Fossil Treasures of the Anza-Borrego Desert*; Jefferson, G.T., Lindsay, L., Eds.; Sunbelt Publications: Chula Vista, CA, USA, 2005; pp. 89–104. ISBN 9780932653505.
25. Shirvell, C.R.; Stockli, D.F.; Axen, G.J.; Grove, M. Miocene-Pliocene exhumation along the west Salton detachment fault, southern California, from (U-Th)/He thermochronometry of apatite and zircon. *Tectonics* **2009**, *28*, 14. [[CrossRef](#)]
26. Umhoefer, P.J.; Darin, M.H.; Bennett, S.E.K.; Skinner, L.A.; Dorsey, R.J.; Oskin, M.E. Breaching of strike-slip faults and successive flooding of pull-apart basins to form the Gulf of California seaway from ca. 8–6 Ma. *Geology* **2018**, *46*, 695–698. [[CrossRef](#)]
27. Steely, A.N.; Janecke, S.U.; Dorsey, R.J.; Axen, G.J. Early Pleistocene initiation of the San Felipe fault zone, SW Salton Trough, during reorganization of the San Andreas fault system. *Bull. Geol. Soc. Am.* **2009**, *121*, 663–687. [[CrossRef](#)]
28. Ruisaard, C.I. Stratigraphy of the Miocene Alverson Formation, Imperial County, California. Master's Thesis, San Diego State University, San Diego, CA, USA, 1979; p. 125. Available online: <https://digitallibrary.sdsu.edu/islandora/object/sdsu%3A235> (accessed on 21 April 2022).
29. Oskin, M.; Stock, J.; Martín-Barajas, A. Rapid localization of Pacific-North American plate motion in the Gulf of California. *Geology* **2001**, *29*, 459–462. [[CrossRef](#)]
30. Oskin, M.; Stock, J. Marine incursion synchronous with plate-boundary localization in the Gulf of California. *Geology* **2003**, *31*, 23–26. [[CrossRef](#)]
31. Van De Kamp, P.C. Holocene continental sedimentation in the Salton Basin, California: A reconnaissance. *Bull. Geol. Soc. Am.* **1973**, *84*, 827–848. [[CrossRef](#)]
32. Dorsey, R.J.; Fluette, A.; McDougall, K.; Housen, B.A.; Janecke, S.U.; Axen, G.J.; Shirvell, C.R. Chronology of Miocene–Pliocene deposits at Split Mountain Gorge, Southern California: A record of regional tectonics and Colorado River evolution. *Geology* **2007**, *35*, 57–60. [[CrossRef](#)]
33. Nicholson, U.A.M. Landscape Evolution and Sediment Routing Across A Strike-Slip Plate Boundary. Ph.D. Thesis, University of Aberdeen, Aberdeen, UK, 2009; p. 475.
34. Robinson, P.J. A Provenance Study of Cenozoic Palaeo-Deltaic Sediments in California as A Tool for Understanding the Evolution of the Colorado River. Ph.D. Thesis, University of Aberdeen, Aberdeen, UK, 2013; p. 425.
35. Thürach, H. Über das vorkommen mikroskopischer zirkone und titanmineralien in des gesteinen. *Verh. Der Phys.-Med. Ges. Zu Würzburg* **1884**, *18*, 203–284.
36. Hedberg, H.D. Some aspects of sedimentary petrology in relation to stratigraphy in the Bolivar coast fields of the Maracaibo Basin, Venezuela. *J. Palaeontol.* **1928**, *2*, 32–42.
37. Illing, V.C. The oilfields of Trinidad. *Proc. Geol. Assoc.* **1916**, *27*, 115.
38. Reed, R.D. Some methods for heavy mineral investigations. *Econ. Geol.* **1924**, *19*, 320–337. [[CrossRef](#)]
39. Tickell, F.G. The correlative value of the heavy minerals. *Am. Assoc. Of. Pet. Geol. Bull.* **1924**, *8*, 158–168.
40. Mange, M.A.; Wright, D.T. (Eds.) *Heavy Minerals in Use*; Elsevier: Amsterdam, The Netherlands, 2007; pp. 439–464.
41. Morton, A.C.; Knox, R.W. O' B.; Hallsworth, C. Correlation of reservoir sandstones using quantitative heavy mineral analysis. *Pet. Geosci.* **2002**, *8*, 251–262. [[CrossRef](#)]
42. Morton, A.C.; Milne, A. Heavy mineral stratigraphic analysis on the Clair Field, UK, West of Shetlands: A unique real-time solution for red-bed correlation while drilling. *Pet. Geosci.* **2012**, *18*, 115–128. [[CrossRef](#)]
43. Mange, M.A.; Maurer, H. *Heavy Minerals in Colour*; Chapman and Hall: London, UK, 2012.
44. Morton, A.C.; Hallsworth, C.R. Identifying provenance-specific features of detrital heavy mineral assemblages in sandstones. *Sediment. Geol.* **1994**, *90*, 241–256. [[CrossRef](#)]
45. Morton, A.C.; Hallsworth, C.R. Processes controlling the composition of heavy mineral assemblages in sandstones. *Sediment. Geol.* **1999**, *124*, 3–29. [[CrossRef](#)]
46. Morton, A.C. A new approach to provenance studies: Electron microprobe analysis of detrital garnets from Middle Jurassic sandstones of the northern North Sea. *Sedimentology* **1985**, *32*, 553–566. [[CrossRef](#)]
47. Rainbird, R.H.; Heaman, L.M.; ANDYoung, G. Sampling Laurentia: Detrital zircon geochronology offers evidence for an extensive Neoproterozoic river system originating from the Grenville orogen. *Geology* **1992**, *20*, 351–354. [[CrossRef](#)]
48. Mange, M.A.; Morton, A.C. Chapter 13: Geochemistry of Heavy Minerals. In *Heavy Minerals in Use*; Mange, M.A., Wright, D.T., Eds.; Elsevier: Amsterdam, The Netherlands, 2007; pp. 345–391.
49. Gerdes, A.; Zeh, A. Combined U–Pb and Hf isotope LA-(MC)-ICP-MS analyses of detrital zircons: Comparison with SHRIMP and new constraints for the provenance and age of an Armorican metasediment in Central Germany. *Earth Planet. Sci. Lett.* **2006**, *249*, 47–61. [[CrossRef](#)]
50. Frei, D.; Gerdes, A. Precise and accurate in situ U–Pb dating of zircon with high sample throughput by automated LA-SF-ICP-MS. *Chem. Geol.* **2009**, *261*, 261–270. [[CrossRef](#)]
51. Sláma, J.; Košler, J.; Condon, D.J.; Crowley, J.L.; Gerdes, A.; Hanchar, J.M.; Horstwood, M.S.; Morris, G.A.; Nasdala, L.; Norberg, N.; et al. Plešovice zircon—A new natural reference material for U–Pb and Hf isotopic microanalysis. *Chem. Geol.* **2008**, *249*, 1–35. [[CrossRef](#)]

52. Nasdala, L.; Hofmeister, W.; Norberg, N.; Martinson, J.; Corfu, F.; Dörr, W.; Kamo, S.; Kennedy, A.; Kronz, A.; Reiners, P.; et al. Zircon M257-a Homogeneous Natural Reference Material for the Ion Microprobe U-Pb Analysis of Zircon. *Geostand. Geoanalytical Res.* **2008**, *32*, 247–265. [[CrossRef](#)]
53. Mattinson, J.M. Analysis of the relative decay constants of ²³⁵U and ²³⁸U by multi-step CA-TIMS measurements of closed-system natural zircon samples. *Chem. Geol.* **2010**, *275*, 186–198. [[CrossRef](#)]
54. Ludwig, K.R. *User's Manual for Isoplot 3.00: A Geochronological Toolkit for Microsoft Excel*; Special Publications; Berkeley Geochronology Center: Berkeley, CA, USA, 2003; p. 4.
55. Rey, F.M.; Olariu, C.; Steel, R.J. Using the modern Colorado delta to reconstruct the compound clinoforms of the Pliocene Colorado delta. *J. Sediment. Res.* **2022**, *92*, 405–432. [[CrossRef](#)]
56. Winker, C.D.; Kidwell, S.M. Stratigraphic evidence for ages of different extensional styles in the Salton Trough, southern California. *Geol. Soc. Am. Abstr. Programs* **2002**, *34*, 884.
57. Cloos, M.E. Detrital Zircon U-Pb and (U-Th)/He Geo-Thermochronometry and Submarine Turbidite Fan Development in the Mio-Pliocene Gulf of California, Fish Creek-Vallecito Basin, Southern California. Ph.D. Thesis, University of Texas Austin, Austin, TX, USA, 2014.
58. Hovius, N. Controls on Sediment Supply by Large Rivers. In *Relative Role of Eustacy, Climate, and Tectonism in Continental Rocks*; Kocurek, G., Ed.; SEPM Special Publication: Tulsa, OK, USA, 1998; Volume 59, pp. 2–16. [[CrossRef](#)]
59. Steckler, M.S.; Akhter, S.H.; Seeber, L. Collision of the Ganges–Brahmaputra delta with the Burma Arc: Implications for earthquake hazard. *Earth Planet. Sci. Lett.* **2008**, *273*, 367–378. [[CrossRef](#)]
60. Stow, D.; Nicholson, U.; Kearsley, S.; Tatum, D.; Gardiner, A.; Ghabra, A.; Jaweesh, M. The Pliocene-Recent Euphrates river system: Sediment facies and architecture as an analogue for subsurface reservoirs. *Energy Geosci.* **2020**, *1*, 174–193. [[CrossRef](#)]
61. Pindell, J.L.; Kennan, L.; Wright, D.; Erikson, J. Clastic domains of sandstones in central/eastern Venezuela, Trinidad, and Barbados: Heavy mineral and tectonic constraints on provenance and palaeogeography. *Geol. Soc. Lond. Spec. Publ.* **2009**, *328*, 743–797. [[CrossRef](#)]
62. George, C.F.; Macdonald, D.I.M.; Spagnolo, M. 2019. Deltaic sedimentary environments in the Niger Delta. *J. Afr. Earth Sci.* **2019**, *160*. [[CrossRef](#)]
63. Udo, I.; Udofia, P.A. Petrography and provenance analysis of conglomeritic lithofacies of the Ameki Formation in the northeastern part of the Niger Delta Basin, Nigeria. *Int. J. Eng. Sci.* **2020**, *9*, 42–55.
64. Fielding, L.; Najman, Y.; Millar, I.; Butterworth, P.; Garzanti, E.; Vezzoli, G.; Barfod, D.; Kneller, B. 2018. The initiation and evolution of the River Nile. *Earth Planet. Sci. Lett.* **2018**, *489*, 166–178. [[CrossRef](#)]
65. Craddock, W.H.; Kylander-Clark, R.C. U-Pb ages of detrital zircons from the Tertiary Mississippi River Delta in central Louisiana: Insights into sediment provenance. *Geosphere* **2013**, *9*, 1832–1851. [[CrossRef](#)]
66. Viviroli, D.; Weingartner, R.; Messereli, B. Assessing the hydrological significance of the world's mountains. *Mt. Res. Dev.* **2003**, *23*, 32–40. [[CrossRef](#)]
67. Syvitski, J.P.M.; Vörösmarty, C.J.; Kettner, A.J.; Green, P. Impact of humans on the flux of terrestrial sediment to the global coastal ocean. *Science* **2005**, *308*, 376–380. [[CrossRef](#)]
68. Fernandes, V.M.; Roberts, G.G.; White, N.; Whittaker, A.C. Continental-scale landscape evolution: A history of North American topography. *J. Geophys. Res. Earth Surf.* **2019**, *124*, 2689–2722. [[CrossRef](#)]
69. Thompson, R.S. Pliocene environments and climates in the western United States. *Quat. Sci. Rev.* **1991**, *10*, 115–132. [[CrossRef](#)]
70. Haywood, A.M.; Dowsett, H.J.; Dolan, A.M. Integrating geological archives and climate models for the mid-Pliocene warm period. *Nat. Commun.* **2016**, *7*, 10646. [[CrossRef](#)] [[PubMed](#)]
71. Laskar, J.; Robutel, P.; Joutel, F.; Gastineau, M.; Correia, A.C.M.; Levrard, B. A long-term numerical solution for the insolation quantities of the Earth. *Astron. Astrophys.* **2004**, *428*, 261–285. [[CrossRef](#)]
72. Becker, J.; Lourens, L.J.; Hilgen, F.J.; Van Der Laan, E.; Kouwenhoven, T.J.; Reichert, G.R. Late Pliocene climate variability on Milankovitch to millennial time scales: A high-resolution study of MIS100 from the Mediterranean. *Palaeogeogr. Palaeoclimatol. Palaeoecol.* **2005**, *228*, 338–360. [[CrossRef](#)]
73. Haywood, A.M.; Dowsett, H.J.; Valdes, P.J.; Lunt, D.J.; Francis, J.F.; Sellwood, B.W. Introduction. Pliocene climate, processes and problems. *Philos. Trans. R. Soc. A* **2009**, *367*, 3–17. [[CrossRef](#)]
74. Galloway, W.E.; Whiteaker, T.L.; Ganey-Curry, P. History of Cenozoic North American drainage basin evolution, sediment yield, and accumulation in the Gulf of Mexico basin. *Geosphere* **2011**, *7*, 938–973. [[CrossRef](#)]
75. Dorsey, R.J.; Lazear, G. A post-6 Ma sediment budget for the Colorado River. *Geosphere* **2013**, *9*, 781–791. [[CrossRef](#)]
76. Sincavage, T.R.; Liang, M.; Pickering, J.; Goodbred, S.; Passalacqua, P. Antecedent topography and sediment dispersal: The influence of geologically instantaneous events on basin fill patterns. *JGR Earth Surf.* **2022**, *127*, 17. [[CrossRef](#)]
77. House, P.K.; Pearthree, P.A.; Howard, K.A.; Bell, J.W.; Perkins, M.E.; Faulds, J.E.; Brock, A.L.; Pederson, J.; Dehler, C.M. *Birth of the Lower Colorado River—Stratigraphic and Geomorphic Evidence for Its Inception Near the Conjunction of Nevada, Arizona, and California: Interior Western United States: Geological Society of America Field Guide*; Geological Society of America: Boulder, CO, USA, 2005; Volume 6, pp. 357–387.
78. House, P.K.; Pearthree, P.A.; Perkins, M.E. *Stratigraphic Evidence for the Role of Lake Spillover in the Inception of the Lower Colorado River in Southern Nevada and Western Arizona: Geological Society of America Special Papers*; Geological Society of America: Boulder, CO, USA, 2008; Volume 439, pp. 335–353.

79. Pearthree, P.A.; House, P.K. Paleogeomorphology and Evolution of the Early Colorado River Inferred from Relationships in Mohave and Cottonwood Valleys, Arizona, California, and Nevada. *Geosphere* **2014**, *10*, 1139–1160. [[CrossRef](#)]
80. Thacker, J.O.; Karlstrom, K.E.; Crossey, L.J.; Crow, R.S.; Cassidy, C.E.; Beard, L.S.; Singleton, J.S.; Strickland, E.D.; Seymour, N.M.; Wyatt, M.R. Post-12 Ma Deformation in the Lower Colorado River Corridor, Southwestern USA: Implications for Diffuse Transtension and the Bouse Formation. *Geosphere* **2019**, *16*, 111–135. [[CrossRef](#)]

Disclaimer/Publisher's Note: The statements, opinions and data contained in all publications are solely those of the individual author(s) and contributor(s) and not of MDPI and/or the editor(s). MDPI and/or the editor(s) disclaim responsibility for any injury to people or property resulting from any ideas, methods, instructions or products referred to in the content.